Carbon emission and export from Ket River, western Siberia

Artem G. Lim[1], Ivan V. Krickov[1], Sergey N. Vorobyev[1],

Mikhail A. Korets[2], Sergey Kopysov[1],

Liudmila S. Shirokova[3], Jan Karlsson[4], and Oleg S. Pokrovsky[5*]

[1]*BIO-GEO-CLIM Laboratory, Tomsk State University, Tomsk, Russia*
[2] *V.N. Sukachev Institute of Forest of the Siberian Branch of Russian Academy of Sciences – separated department of the KSC SB RAS, Krasnoyarsk, 660036, Russia*
[3] *N. Laverov Federal Center for Integrated Arctic Research, Russian Academy of Sciences, Arkhangelsk, Russia*
[4]*Climate Impacts Research Centre (CIRC), Department of Ecology and Environmental Science, Umeå University, Linnaeus väg 6, 901 87 Umeå, Sweden.*
[5] *Geosciences and Environment Toulouse, UMR 5563 CNRS, 14 Avenue Edouard Belin 31400 Toulouse, France*

Key words: CO_2, C, emission, boreal, river, export, landscape, Siberia

* email: oleg.pokrovsky@get.omp.eu

Abstract

Despite recent progress in the understanding of the carbon (C) cycle of Siberian permafrost-affected rivers, spatial and seasonal dynamics of C export and emission from medium-size rivers (50,000 - 300,000 km² watershed area) remain poorly known. Here we studied one of the largest tributaries of the Ob River, the Ket River (watershed = 94,000 km²) which drains through pristine taiga forest of the boreal zone in western Siberian Lowland (WSL). We combined continuous and discrete measurements of carbon dioxide (CO_2) concentration using submersible CO_2 sensor and floating chamber flux (FCO_2), with methane (CH_4), organic and inorganic C (DOC and DIC, respectively), particulate organic C and total bacterial concentrations over a 800-km transect of the Ket River main stem and its 26 tributaries during spring flood (May 2019) and 12 tributaries during summer baseflow (end of August – beginning of September 2019). The partial pressure of CO_2 (pCO_2) was lower and less variable in the main stem (2000 to 2500 µatm) compared to that in tributaries (2000 to 5000 µatm). In the tributaries, the pCO_2 was 40 % higher during baseflow compared to spring flood, whereas in the main stem, it did not vary significantly across the seasons. The methane concentration in the main stem and tributaries was a factor of 300 to 1900 (flood period) and 100 to 150 times lower than that of CO_2, and ranged from 0.05 to 2.0 µmol L^{-1}. The FCO_2 ranged from 0.4 to 2.4 g C m^{-2} d^{-1} in the main channel and from 0.5 to 5.0 g C m^{-2} d^{-1} in the tributaries, being the highest during August in tributaries and weakly dependent on season in the main channel. During summer baseflow, the DOM aromaticity, bacterial number, and needleleaf forest coverage of the watershed positively affected CO_2 concentrations and fluxes. We hypothesize that relatively low spatial and seasonal variability in FCO_2 of the Ket River is due to flat homogeneous landscape (bogs and taiga forest) that results in long water residence times and stable input of allochthonous DOM, which dominate the FCO_2. The open water period (May to October) C emission from the fluvial network (main stem and tributaries) of the Ket River was estimated to 127±11 Gg C y^{-1} which is lower than the downstream dissolved and particulate C export during the same period. The estimated fluvial C emissions are highly conservative and contain uncertainties, linked to ignoring hot spots and hot moments of emissions, notably in the floodplain zone. This stresses the need of improving temporal resolution of FCO_2 and water coverage across seasons and emphasizes the important role of WSL rivers for release of CO_2 to the atmosphere.

Introduction

Assessment of greenhouse gas (GHG) emission from rivers is crucially important for understanding the C cycle under various climate change scenarios (Campeau and del Giorgio, 2014; Chadburn et al., 2017; Tranvik et al., 2018; Vonk et al., 2019; Vachon et al., 2020). Rivers receive terrestrial C and process and emit a significant share of this C during transit to the sea (Liu et al., 2022). Quantifications of riverine C emissions are sufficiently robust for relatively well studied regions of the world such as the European and N American boreal zone (Dawson et al., 2004; Dinsmore et al., 2013; Wallin et al., 2013; Leith et al., 2015; Zolkos et al., 2019; Hutchins et al., 2020), or Arctic and subarctic rivers of Alaska (Striegl et al., 2012; Crawford et al., 2013; Stackpoole et al., 2017), although subjected to great uncertainty. Despite significant progress in assessing riverine pCO_2 in previously under-represented or ignored regions such as lotic systems of Asia (Ran et al., 2015, 2017; Varol and Li, 2017) or South America (Almeida et al., 2017), these studies generally use a combination of pH and alkalinity (DIC) to calculate the pCO_2 instead of direct in-situ measurements, alike the studies of global emissions (Raymond et al., 2013; Lauerwald et al., 2015). At the same time, there is a growing number of studies reporting directly measured riverine pCO_2 – either discretely (Alin et al. 2011; Borges et al., 2015; Amaral et al. 2018; 2022; Leng et al. 2022), continuously at fixed sites (Crawford et al. 2016a, Schneider et al. 2020; Gómez-Gener et al. 2021a), or along the river flow (Abril et al. 2014; Crawford et al. 2016b; 2017; Borges et al. 2019). However, these studies are limited to tropical and temperate zones of the world, and boreal regions of Western Europe and Northern America, and thus, further continuous and discrete measurements of CO_2 concentration and fluxes in rivers from under-represented regions such as Northern Eurasia are needed.

Indeed, despite their currently sub-ordinary role in global riverine CO_2 emissions (30% temperate, 13% Arctic regions, Liu et al., 2022), high latitude regions are important because of their large C stocks, partly located in the permafrost, and their extreme vulnerability to observed and projected warming, which can release 80 Pg C upon abrupt thaw and up to 200 Pg C upon gradual thaw by 2300 (Turetsky et al., 2020). This is especially true for Siberia, hosting large C stocks in soils and wetlands intersected by extensive river networks that deliver majority of water and C to the Arctic Ocean (Feng et al., 2013). There has been substantial progress in quantification of carbon export and emissions from Siberian permafrost-affected rivers

(Lobbes et al., 2000; Raymond et al., 2007; Cooper et al., 2008; Semiletov et al., 2011; Feng et al., 2013; Griffin et al., 2018; Wild et al., 2019). However, spatial and seasonal features of C export and emission from tributaries of Siberian rivers are still remain poorly known. Existing data (Denfeld et al., 2013; Serikova et al., 2018; Karlsson et al., 2021; Vorobyev et al., 2021) suggest that C (predominantly as CO_2) emissions from Siberian rivers can vary largely over space and time. Such high variations do not allow reliable quantitative assessment of C emission and integrating these values into regional and global C models.

In order to better understand and constrain the magnitude of C emission from Siberian rivers, we studied the Ket River (watershed 94,000 km²), a typical tributary of the Ob River in western Siberia. The Ob river is the largest (in terms of watershed area) Siberian river and drains large pristine territories of taiga forest and bogs. The catchment of Ob includes extensive regions of permafrost but a major part of it (80 %) is situated in the permafrost-free zone of which very few data exist on riverine C emissions (Karlsson et al., 2021). The Ket river drains through dense southern taiga forest and abundant wetlands with almost no human activity, thus serving a representative system for understanding C cycling in permafrost-free Siberian rivers. We followed, via a boat routing over the main stem and main tributaries of the river, the in-situ CO_2 concentrations combined with discrete sampling for dissolved CH_4, DOC, DIC, total bacterial number and particulate organic matter. These measurements were complemented with regular floating chamber measurements of CO_2 emission fluxes. We performed these observations during two main open water seasons of the year - the peak of the spring flood and the end of the summer baseflow. Our first objective was to quantify the difference in C concentration and emission during two seasons for the main steam and the tributaries and to relate these differences to main physico-chemical parameters of the water column and physio-geographical parameters (land cover) of the river watersheds. Our second objective was to obtain total C emission flux from the river watershed area and compare it to downstream export yield of dissolved and particulate carbon.

2. Study Site, Materials and Methods

2.1. Ket River and its tributaries

The Ket River main stem and its 26 tributaries sampled in this study include watersheds of distinct sizes (catchment area ranged from 94,000 at the Ket's mouth to 20 km² of smallest tributary), but rather similar lithology, climate and vegetation (**Fig. 1, Table S1**). This poorly accessible river basin is fully pristine (50 % forest, 40 % wetlands), and has almost no agricultural and forestry activity. The watershed of Ket has very low population density (0.27 person km^{-2}) and lacks road infrastructure due to absence of oil and gas development and production. In this regard, this river can serve as a model for medium size bog-forest rivers of the western Siberia Lowland and results obtained from this watershed can be extrapolated to much larger territory, comprising about 1 million km^2 of permafrost-free taiga forest and bog regions of the southern part of WSL.

The mean annual air temperatures (MAAT) is -0.7 ± 0.1 °C and the mean annual precipitation is 520 ± 20 mm y^{-1} in the central part of the basin. The lithology of this part of western Siberian lowland is dominated by Pleistocene silts and sands with carbonate concretions overlayed by quaternary deposits (loesses, fluvial, glacial and lacustrine deposits). The dominant soils are podzols in forest areas and histosols in peat bog regions. Further description of climate, lithology and landscape features of the territory is provided in former studies (Frey and Smith, 2007; Pokrovsky et al., 2015).

The peak of annual discharge in 2019 occurred in the end of May; in August, the discharge was 3 to 5 times smaller (**Fig. 1**). Note that low runoff, lack of relief and highly homogenous landscape coverage of the permafrost-free zone of western Siberia in general and of the Ket River basin in particular provide quite smooth hydrographs of the rivers. In this regard, the spring flood period is extended over 2 months, from the beginning of May to middle of July, whereas summer baseflow includes second half of July, August and September. As a result, similar to previous study of rivers along a 2500 km transect of the WSL territory, the timing of the two sampling campaigns covered approximately 80% of the annual water discharge in the basins (Serikova et al., 2018). From May 18 to May 28, 2019, and from August 30 to September 2, 2019, we started the boat trip in the middle course of the Ket River (Beliy Yar), and moved, first, 475 km upstream the Ket river till its most headwaters, and then moved 834 km downstream till the river mouth, with an average speed

of 20 km h^{-1}. During summer baseflow, the 4-days trip was shortened by 200 km due to too low water level in the upper reaches of the main stem and some small tributaries. We stopped each 30-50 km along the Ket River and sampled for major hydrochemical parameters, GHG, river suspended matter and total bacterial number of the main stem. We also moved several km upstream of selected tributaries to record CO_2 concentrations for at least 1 h and to sample for river hydrochemistry. At several occasions during spring flood, we monitored CO_2 concentration and performed chamber measurements in the main stem and tributaries during both day and night time period.

2.2. CO_2 and CH_4 concentrations and CO_2 fluxes by floating chambers

Surface water CO_2 concentration was measured continuously, *in-situ* by deploying a portable infrared gas analyzer (IRGA, GMT222 CARBOCAP® probe, Vaisala®; accuracy ± 1.5%) of two ranges (2 000 and 10 000 ppm) as described in previous work of our group on the Lena River (Vorobyev et al., 2021). Sensor preparation was conducted in the lab following the method described by Johnson et al. (2009). The measurement unit (MI70, Vaisala®; accuracy ± 0.2%) was connected to the sensor allowing instantaneous readings of pCO_2. The sensors were calibrated in the lab against standard gas mixtures (0, 800, 3 000, 8 000 ppm; linear regression with $R^2 > 0.99$) before and after the field campaign. The sensors' drift was 0.03-0.06% per day and overall error was 4-8% (relative standard deviation, RSD). Following calibration, post-measurement correction of the sensor output induced by changes in water temperature and barometric pressure was done by applying empirically derived coefficients following Johnson et al. (2009). These corrections never exceeded 5% of the measured values. During the cruise, we routinely measured atmospheric CO_2 with the probe as a check for its good functioning. Furthermore, we tested two different sensors in several sites of the river transect: a main probe used for continuous measurements and another probe used as a control and never employed for continuous measurements. We did not find any sizable (>10%) difference in measured CO_2 concentration between these two probes.

The probe was enclosed within a waterproof and gas-permeable membrane. For this, we used a protective expanded polytetrafluoroethylene (PTFE) sleeve that is highly permeable to CO_2 but impermeable to water (Johnson et al., 2009). The sensor was placed into a tube which was submerged 0.5 m below the

168 water surface. A Campbell logger was connected to the system allowing continuous recording of the CO_2
169 concentration, water temperature and pressure every minute. These readings were averaged over 10 minute
170 intervals yielding 732 individual pCO_2, water temperature and pressure values. The CO_2 concentrations in the
171 Ket River tributaries included between 10 and 20 averaged pCO_2 values for each tributary (250 measurements
172 in total) during spring flood period. In addition to continuous *in-situ* CO_2 measurements, we estimated pCO_2
173 via measured pH and DIC values, using the set of constants typically applied for riverine pCO_2 estimation in
174 organic-rich waters (Cai and Wang, 1998; DelDuco and Xu, 2017). The U-test (Mann-Whitney) demonstrated
175 a lack of significant difference in CO_2 concentrations measured by Vaissala and calculated from the pH and
176 DIC of the river water.

177 For CH_4 analyses, unfiltered water was sampled in 60-mL Serum bottles. For this, the bottles and caps
178 were manually submerged at approx. 30 cm depth from the water surface. The bottles were closed without
179 air bubbles using vinyl stoppers and aluminum caps and immediately poisoned by adding 0.2 mL of saturated
180 $HgCl_2$ via a two-way needle system. The samples were stored approximately one week in the refrigerator
181 before the analyses. In the laboratory, a headspace was created by displacing approximately 40% of water
182 with N_2 (99.999%). Two 0.5-mL replicates of the equilibrated headspace were analyzed for their
183 concentrations of CH_4, using a Bruker GC-456 gas chromatograph (GC) equipped with flame ionization and
184 thermal conductivity detectors (Serikova et al., 2019; Vorobyev et al., 2021). After every 10 samples, a
185 calibration of the detectors was performed using Air Liquid gas standards (i.e. 145 ppmv). Duplicate injection
186 of the samples showed that results were reproducible within ±5%. The specific gas solubility for CH_4
187 (Yamamoto et al., 1976) were used in calculation of the CH_4 content in the water.

188 Discrete CO_2 fluxes were measured by using two floating CO_2 chambers equipped with non-
189 dispersive infrared SenseAir® CO_2 loggers (Bastviken et al., 2015), at each of the 7 (spring flood) and 6
190 (summer baseflow) sampling location of the main stem and 26 tributaries following the procedures described
191 elsewhere (Serikova et al., 2019; Krickov et al., 2021). The chambers were not anchored but slowly free-
192 drifted together with the boat, because it is known that anchored chambers can artificially enhance fluxes due
193 to turbulence thus providing erroneous estimates (Lorke et al., 2015). The CO_2 accumulation rate inside each
194 chamber was recorded continuously at 300 s interval. We used first 0.5–1 h of measurements for computing

CO_2 accumulation rate inside each chamber by linear regression. In addition to *in-situ* chamber measurements, CO_2 fluxes were calculated from wind speed and surface water gas concentrations using standard approaches (Guérin et al., 2007; Wanninkhof, 1992; Cole and Caraco, 1998). This technique is based on the two-layer model of Liss and Slater (1974), and widely used for GHG flux assessment (Repo et al. 2007; Laurion et al. 2010; Elder et al. 2018). The gas transfer coefficient was taken from Cole and Caraco (1998):

$$k_{600} = 2.07 + 0.215 \cdot {U_{10}}^{1.7} \quad (1)$$

where U_{10} is the wind speed taken at 10 m height. Average daily wind speed was retrieved from official data of the nearest weather station (Belyi Yar town) as published by Rosgidromet for the day of sampling. The gas transfer velocity was calculated in two ways - assuming zero wind speed and the actually measured wind speed at the site of sampling or at the Belyi Yar town, middle course of the Ket River. For comparison with previous estimates in large Siberian rivers (Karlsson et al., 2021; Vorobyev et al., 2021), we also used a gas transfer velocity of 4.46 m d^{-1} measured in the 4 largest rivers of Western Siberia Lowalnd (WSL) in June 2015 (Ob', Pur, Pyakupur and Taz rivers, Karlsson et al., 2021) which is representative for large lowland rivers (Alin et al., 2011; Beaulieu et al., 2012).

2.3. Chemical analyses of the river water

The dissolved oxygen (CellOx 325; accuracy of ±5%), specific conductivity (TetraCon 325; ±1.5%), and water temperature (±0.2 °C) were measured in-situ at 20 cm depth using a WTW 3320 Multimeter. The pH was measured using portable Hanna instrument via combined Schott glass electrode calibrated with standard buffer solutions (4.01, 6.86 and 9.18 at 25°C), with an uncertainty of 0.01 pH units. The temperature of buffer solutions was within ± 2°C of that of the river water. The water was sampled in pre-cleaned polypropylene bottle from 20-30 cm depth in the middle of the river and immediately filtered through disposable single-use sterile Sartorius filter units (0.45 µm pore size). The first 50 mL of filtrate was discarded. The DOC and Dissolved Inorganic Carbon (DIC) were determined by a Shimadzu TOC-VSCN Analyzer (Kyoto, Japan) with an uncertainty of 3% and a detection limit of 0.1 mg/L. Blanks of MilliQ water passed through the filters demonstrated negligible release of DOC from the filter material. The SUVA was

measured via ultraviolet absorbance at 254 nm using a 10-mm quartz cuvette on a Bruker CARY-50 UV-VIS spectrophotometer.

The concentration of C and N in suspended material (Particulate Organic Carbon and Nitrogen (POC and PON, respectively)) was determined via filtration of 1 to 2 L of freshly collected river water (at the river bank or in the boat) with pre-weighted GFF filters (47 mm, 0.45 µm) and Nalgene 250-mL polystyrene filtration units using a Mityvac® manual vacuum pump. Particulate C and N were measured using catalytic combustion with Cu-O at 900°C with an uncertainty of ≤ 0.5% using Thermo Flash 2000 CN Analyzer at EcoLab, Toulouse. The samples were analyzed before and after 1:1 HCl treatment to distinguish between total and inorganic C; however the ratio of $C_{organic}$: $C_{carbonate}$ in the river suspended matter (RSM) was always above 20 and the contribution of carbonate C to total C in the RSM was equal in average 0.3±0.3% (2 s.d., n = 30).

Total microbial cell concentration was measured after sample fixation in glutaraldehyde, by a flow cytometry (Guava® EasyCyteTM systems, Merck). Cells were stained using 1 µL of a 10 times diluted SYBR GREEN solution (10000x, Merck), added to 250 µL of each sample before analysis. Particles were identified as cells based on green fluorescence and forward scatter (Marie et al., 2001).

2.4. Riverine carbon export flux by the Ket catchment

The C export flux over active (unfrozen) period (May to October) from the Ket basin was calculated based on monthly-averaged discharge at the river mouth in 2019 available from Russian Hydrological Survey and DOC, DIC and POC concentrations measured in the low reaches of the Ket River in this study (see hydrograph in **Fig. 1**). Riverine element fluxes should be usually estimated using a LOADEST method (Holmes et al., 2012) from calculated daily element loads. The latter typically obtained from a calibration regression, applied to daily discharge. This calibration regression can be constructed from time series of paired streamflow and measured element concentration data for sufficient period of the year. In our previous works in this and other similar boreal regions, we demonstrated that this method provides reasonable (within 10 to 30 %) agreement with monthly export fluxes calculated by multiplying mean monthly discharge by mean monthly concentration (Chupakov et al., 2020; Pokrovsky et al., 2022; Vorobyev et al., 2019). Given

that the intrinsic uncertainties on mean monthly discharge are also between 10 and 20 % (see discussion for the WSL rivers in Pokrovsky et al., 2020), in this study, for open-water period export flux calculation, we used DOC, DIC and POC concentrations measured during spring flood (for May and June period) and baseflow (for August, September and October period). For the month of July, we used the mean concentrations of end of May and August-September which is in accord with seasonal discharge pattern of the Ket River. Note that the contribution of non-studied October month to total open water period water flux is < 10 % and thus cannot provide sizable uncertainties

2.5. Landscape parameters and water surface area of the Ket River basin

The physio-geographical characteristics of the 26 Ket tributaries and the 7 points of the Ket main stem (**Table S1, Fig. S1**) were determined by applying available digital elevation model (DEM GMTED2010), soil, vegetation and lithological maps. The landscape parameters were typified using TerraNorte Database of Land Cover of Russia (Bartalev et al., 2020; http://terranorte.iki.rssi.ru). This included various type of forest (evergreen, deciduous, needleleaf/broadleaf), grassland, tundra, wetlands, water bodies and riparian zones. Note that the land cover data correspond to the whole catchment area upstream of the sampling point. The climate parameters the watershed were obtained from CRU grids data (1950-2016) (Harris et al., 2014) and NCSCD data (Hugelius et al., 2013), respectively. The biomass was obtained from BIOMASAR2 dataset in raster format with spatial resolution of 1 x 1 km (Santoro et al., 2010). The soil OC content was taken from the Northern Circumpolar Soil Carbon Database (NCSCD). The original NCSCD dataset produced in GIS vector format corresponding to 1:1,000,000 scale of topographic map. It could be rasterized to 1 x 1 km pixel resolution. The lithology layer was taken from GIS version of Geological map of the Russian Federation (scale 1:5,000,000, http://www.geolkarta.ru/). We quantified river water surface area using the global SDG database with 30 m² resolution (Pekel et al., 2016) including both seasonal and permanent water for the open water period of 2019 and for the multiannual average (reference period 2000-2004). We also used a more recent GRWL Mask Database which incorporates first order temporary non-active streams (Allen and Pavelsky, 2018).

2.6. Data analysis

Carbon concentrations and fluxes for all dataset were tested for normality using a Shapiro-Wilk test. In case if the data were not normally distributed, we used non-parametric statistics. Comparisons of GHG parameters in the main stem and tributaries during two sampling seasons were conducted using a non-parametric Mann Whitney test at a significance level of 0.05. For comparison of unpaired data, a non-parametric H-criterion Kruskal-Wallis test was used to reveal the differences between different study sites. The Pearson rank order correlation coefficient ($p < 0.05$) was used to determine the relationship between CO_2 concentrations and emission fluxes and main landscape parameters of the Ket River tributaries, as well as other potential drivers such as pH, O_2, water temperature, specific conductivity, DOC, DIC, particulate carbon and nitrogen, and total bacterial number.

Further identification of C pattern drivers in river waters included a Principal Component Analysis which allowed to test the effect of various hydrochemical and landscape parameters on CO_2 and CH_4 concentrations and CO_2 emissions. In addition to PCA, a Redundancy analysis (RDA) was used to extract and summarize the variation in C pattern that can be explained by a set of explanatory variables (environmental, climatic and hydrochemical factors). The RDA combines a PCA and multiple regression analysis and it was run in XLSTAT is a statistical software that works as an add-on to Excel.

3. Results

3.1. Greenhouse gases and dissolved and particulate C

The main hydrochemical parameters and greenhouse gases concentration and exchange fluxes of the Ket River and its tributaries are listed in **Table 1** and primary data are provided in **Table S2** of the Supplement. Continuous pCO_2 measurements in the main stem during the spring (764 individual data points over the full distance of the boat route (834 km), demonstrated a lack of systematic change in CO_2 concentration from headwaters to the mouth. The CO_2 concentration in tributaries was generally higher than that in the main stem. As a result, the pCO_2 changed by a factor of 1.5 to 2 when tributaries with high CO_2 concentrations join the main stem (**Fig. 2 A**). There were strong but non-systematic variations in CO_2

concentration in the tributaries during the summer (**Fig. 2 C**). The CH_4 concentration (**Table 1 and Fig. S2 A, B**) was low in the Ket River (around 0.17 and 0.86 µmol L^{-1} in May and August, respectively) and in the tributaries (range 0.09 to 2.57 µmol L^{-1}, 2 to 3 times higher values during the baseflow). These values are consistent with the range of CH_4 concentration in other Siberian Rivers such as Lena (0.03 to 0.199 µmol L^{-1}, Bussman, 2013; Vorobyev et al., 2021). In the Ket River main stem and tributaries, the CH_4 concentrations are 300-2000 and 100-150 times lower than those of CO_2 during spring and summer, respectively, and ranged from 0.05 to 2.0 µmol L^{-1}. Consequently, diffuse CH_4 emissions (**Table 1, Fig. S2 C, D)** constituted 0.1 to 0.5% of total C emissions and are not discussed in further detail.

During spring flood, CO_2 fluxes ranged from 0.26 to 3.2 g C m^{-2} d^{-1} in the main stem and tributaries (**Table 1; Fig. 2 B**). During baseflow, the flux in the tributaries varied from 0.37 to 7.4 g C m^{-2} d^{-1} and was a factor of 2 to 3 higher than that in the main stem (**Fig. 2 D; Table 1**). The CO_2 concentration in the river water and gas transfer velocity assessed from discrete measurements by floating chambers (K_T = 0.08-1.83 m d^{-1} in the main stem; 0.2-1.86 m d^{-1} in the tributaries, **Table 1**) allowed for calculation of the continuous CO_2 fluxes (**Fig. 2 B**). For this, we used an average value of K_T between two chamber sites (separated by a distance of 50 to 100 km) to calculate the FCO_2 from in-situ measured pCO_2 in the river section between these two sites. Note that the wind calculated flux was 1.5 to 2 times higher than that measured by chambers, although in 30 % of cases, the wind-speed calculated fluxes were similar to or lower than those measured by floating chambers. The calculation with K_T = 4.46 m d^{-1} (the value typical for large Siberian rivers) overestimated the flux by a factor of 3.7 to 6.0 (**Table S2** of the Supplement). In both cases, the overestimation of calculated flux relative to chamber-measured flux was most pronounced in the tributaries rather than in the main stem.

The DIC concentration increased 5 to 10 times between the spring (2.4 to 2.8 mg L^{-1}) and summer baseflow (18 to 20 mg L^{-1}) and the pH increased by 0.5-0.7 units between spring freshet and summer baseflow (**Fig. 3** and **Fig. S3 A, B** of the Supplement). The DOC concentration ranged from 18 to 25 mg L^{-1} during flood and from 15 to 18 mg L^{-1} during baseflow (**Fig. 3**). There was no systematic variations in DOC concentration over the 834 km of the main stem (20.7 ± 3.6 and 15.0 ± 1.4 mg L^{-1} in May and August, respectively); however, it was slightly higher and more variable in the tributaries (22.0± 4.0 and 16.5 ± 7.4

329 mg L^{-1}, **Fig. S3 C, D)**. The $SUVA_{254}$ remained highly stable throughout the seasons for both the tributaries
330 and the main stem (range from 4.2 to 4.9 L mg C^{-1} m^{-1}, **Table 1**). The POC was 3 times higher during baseflow
331 compared to spring and ranged from 2 to 10 mg L^{-1} (**Fig. 3** and **Fig. S3 E, F**). The total bacterial number
332 ranged from 5.0×10^5 to 8.7×10^5 cells mL^{-1} for the main stem and tributaries without significant ($p > 0.05$)
333 seasonal variation (**Fig. 3** and **S3 G, H**).
334
335 *3.2. Diurnal and spatial variation in CO_2 concentration and flux*
336 The diel (day/night) measurements of CO_2 concentrations have been performed on six tributaries of
337 the Ket River during the spring flood period (**Fig. 4**). In two of them (Sochur ad Lopatka), we measured both
338 CO_2 concentration and CO_2 fluxes via floating chambers. Continuous CO_2 concentrations exhibited a
339 variation between 5 and 25% of the average value. Only in the case of a small tributary Segondenka (**Fig. 4**
340 **E**), when we measured CO_2 over 38 h, there was a local maximum in concentration between 6 and 7 pm
341 during the first and second day of monitoring, without any significant link to the water temperature. The
342 deviation of FCO_2 from the average value over the period of observation in two tributaries (**Fig. 4 A, B**) did
343 not exceed 20%, without any detectable difference between day and night period.
344 The spatial variation in pCO_2 and FCO_2 were tested during spring time in the flood zone of the Ket
345 River middle course, where the flood zone was connected to the main channel. Regardless of the distance
346 from the main stem and the size of the water body, the variation in pCO_2 and chamber-based fluxes were
347 within 30% of the values measured in the main stem. This suggests that the main stem parameters can be used
348 for upscaling the C emissions to the overall flood plain during May, provided that the water bodies are
349 connected to the rivers. Further tests of spatial variation were performed on selected small tributaries, when
350 we moved 8 to 16 km upstream towards the headwaters and monitored the CO_2 concentration in the river
351 water. There was no sizable trend in CO_2 concentration over several km length of the tributary, consistent
352 with small fluctuations over the hundred km-scale of the main stem (**Fig. S4 A**). Altogether, rather minor
353 spatial and diel variations in both CO_2 concentration and emission fluxes support the chosen sampling strategy
354 and allow reliable extrapolation of obtained results to full surface of lotic waters of the Ket River basin, during
355 open water period.

3.3. Impact of water chemistry and catchment characteristics on CO_2 concentrations and emissions

There were generally no strong correlations between CO_2 and CH_4 and the main parameters of the water column (DOC, DIC, POC, TBC and SUVA (**Table 2**). The CO_2 concentration negatively correlated with O_2 concentration ($R_{Pearson}$ = -0.68, $p < 0.05$) and FCO_2 positively correlated with $SUVA_{254}$ ($R = 0.34$, $p < 0.05$), **Fig. 5 A, B**. Other hydrochemical characteristics of the water column did not impact CO_2 and CH_4 concentration and CO_2 flux. During spring flood, there was no positive correlation between FCO_2 of the river water and various hydrochemical characteristics. During the summer baseflow, there were positive correlations between CO_2 concentration or flux and SUVA and total bacterial number (**Table 2**).

Among different landscape factors, only deciduous light needleleaf forest (larch trees) exhibited significant ($p < 0.01$) positive correlations ($0.6 \leq R_S \leq 0.7$) with CO_2 concentration and flux of the Ket River main stem and tributaries, detectable only during the summer baseflow period (**Fig. 5 C**). The peatland and bogs at the watershed exhibited only weak, although positive ($0.2 < R_S < 0.4$), correlation with pCO_2 and FCO_2 (**Table 2**). The other potentially important landscape factors of the river watershed (type of forest, riparian and total aboveground vegetation, recent burns, water bodies) as well as lithological parameters (clays, silts, sands with or without of the presence of carbonate concretions) did not significantly impact the CO_2 and CH_4 concentration and measured CO_2 fluxes in the Ket River basin (**Table 2**). The mean annual precipitation (MAP) at the watershed positively correlated with pCO_2 and FCO_2 during the baseflow (**Fig. 5 D**).

Principal Component Analysis (PCA) demonstrated a general lack of control of physico-chemical parameters of the water column and watershed land cover on C emission pattern in the river waters. The PCA identified two factors that had generally low ability to describe the variance (19 and 7%, respectively; **Table S3** of the Supplement). None of the factors acted significantly on dissolved CO_2, CH_4 or CO_2 flux in the river water. The RDA treatment did not provide additional insights into environmental control of C pattern across the rivers and seasons. After normalization, the main result was that the analyses are not statistically significant ($p > 0.05$).

3.4. Areal C emissions and export fluxes

The C emissions (> 99.5 % CO_2, < 0.5 % CH_4) from the lotic waters of the Ket River basin were assessed based on total river water coverage of the Ket watershed in 2019 (856 km², of which 691 km² is seasonal water, according to the Global SDG database). Given that the measurements were performed at the peak of spring flood in 2019, we used the maximal water coverage of the Ket River basin to calculate the emissions during May and June, and baseflow measurements for July-October period.

For C emission calculation, we used the mean values of FCO_2 of the main stem and the tributaries (1.31±0.81 g C m^{-2} d^{-1} for spring flood; 2.11±1.86 g C m^{-2} d^{-1} for summer-autumn baseflow) which covers full variability of both tributaries and the Ket River main channel (**Table 1, Figure 3**). For the month of July which was not sampled in this work and which represents a transition period between the flood and the baseflow, we used the mean value of May and August (1.55 g C m^{-2} d^{-1}). For the two months of maximal water flow (May - June), the C emission from the whole Ket basin amounts to 68±42 Gg. When summed up with July (25±20 Gg) and summer-autumn baseflow period (August to October) emission (32±28 Gg), the total open water season emission flux is 125 Gg. The uncertainty on the total emission over 6 months of the open water period is difficult to quantify but it can be estimated as between 30 and 50 %. This range covers both the uncertainty of the water coverage of the territory (i.e., Krickov et al., 2021) and the seasonal and spatial variations of CO_2 emission in the Ket basin assessed in the present study.

Based on yield calculations described in section 2.4, the total annual (excluding ice-covered period) riverine C export from the Ket River basin ($S_{watershed}$ = 94,000 km²) is 0.35 Tg (3.7 t C km^{-2}_{land} y^{-1}), of which DOC, DIC and POC accounts for 56, 24 and 20%, respectively. Therefore, over the 6 month of open water period, the C emissions from lotic waters of Ket watershed constituted less than 30% of the dissolved and particulate downstream export of carbon.

4. DISCUSSION

4.1. Temporal and spatial pattern of CO_2 emissions from the river waters

The first important result of the present study is quite low spatial and seasonal variability in both CO_2 concentration and emissions, as well as in DOC concentration and aromaticity (reflected by $SUVA_{254}$) in the main channel (**Fig. 3, S3, Table 1**). The variability in the tributaries was much larger, with differences in dissolved and gaseous C parameters between spring flood and summer-autumn baseflow (**Table S4 A**). While CO_2 concentrations were different between tributaries and the main stem during both flood and baseflow, the CO_2 flux was not different between the main stem and tributaries regardless of season (**Table S4 B**). This, together with lack of diel variations in CO_2 concentrations and emissions during spring period of maximal water coverage (**Fig. 4**), suggest rather stable pattern of CO_2 in the river water, not linked to short-scale processes (primary productivity, photolysis, daily temperature variation). Indeed, negligible primary productivity in the water column may stem from low water temperatures (9.3 °C), shallow photic layer of organic-rich waters (DOC of 22 mg L^{-1}) and lack of periphyton activity during high flow of the spring flood. Note that this finding contrasts the recent results of high frequency pCO_2 measurements in temperate rivers that show a 30 % higher nocturnal emission compared to daytime observations (Gómez-Gener et al., 2021b). At the same time, several studies in tropical DOM-rich rivers such as Congo (Borges et al. 2019) have not detected diel variations of CO_2 because aquatic pelagic primary production was low (Descy et al., 2018) due to strong light attenuation in the water column by DOM.

Concerning spatial variability of C concentrations and emissions during the spring flood, the pCO_2 did not demonstrate sizable variation along the main stem of the Ket River and some of its tributaries, when moving from the mouth to the headwaters. The SUVA also remained highly stable along the river flow. This, together with a lack of FCO_2 correlation with river watershed area during this period (**Table 2**), suggest relatively modest control of headwater C cycling by 'fresh' unprocessed organic matter from upland mire waters on CO_2 emissions from the Ket River tributaries. Much stronger control of mire waters is reported in boreal zone of the Northern Europe (Wallin et al., 2013, 2018). Furthermore, our results on the Ket River main stem and tributaries are in contrast to the general view of disproportional importance of headwater streams in overall CO_2 emission from river basins (Li et al., 2021). A likely explanation is relative low values

of gas transfer velocity measured in the small streams of the Ket basin in this study (0.2 - 2.0 m d^{-1}, **Table 1**). Although these values are totally consistent with transfer coefficients for western Siberia calculated by Liu et al. (2022) based on reach-slope and flow velocity (i.e., ≤ 2 m d^{-1}), they are typical of lakes rather than rivers (i.e., Kokic et al., 2015) and stem from low flow rate, strongly forested and wind-protected river bed without distinct valley due to generally flat orographic context of this part of the WSL (Serikova et al., 2018).

It is worth noting that the overestimation of calculated flux relative to chamber-measured flux was most pronounced in the tributaries rather than in the main stem. Overall, due to small size and short fetch of the Ket River and its tributaries (see pictures of typical environments in **Fig. S4 B-D** of the Supplement), we believe that lower values of K_T are more pertinent to the studied river basin, which has extended flood zone. This is consistent with observations in other flooded regions, where a canopy of vegetation protects the water-air interface from wind stress thus rendering the gas transfer velocity lower compared to open water such as large river (i.e., Foster-Martinez and Variano, 2016; Ho et al., 2018; Abril and Borges, 2019). We therefore warn against the use of high value of transfer velocity, suitable for large rivers of the boreal zone, for assessing the emissions in medium and small size, sheltered streams with extensive riparian vegetation. Another important aspect linked to C emissions from flooded forest (notably birch trees, see **Fig. S4 B**) of the floodplain (e.g. Pangala et al., 2017), not investigated in this study.

4.2. Environmental factors possibly controlling CO_2 concentration and emission pattern in the Ket River main stem and tributaries

Despite sizable variability of pCO_2 in the tributaries, especially during the baseflow, there were no correlations between either pCO_2 or FCO_2 and main hydrochemical parameters of the water column (**Table 2**). The only exception is O_2 concentration, which negatively correlated with pCO_2 during spring flood and both pCO_2 and FCO_2 during summer baseflow (**Fig. 5 A**). This finding suggests potential importance of shallow suboxic riparian flooded zone, meadows and forest, as well as floodplain lakes, in controlling CO_2 build up in the water column due to diffusion from sediments or decaying macrophytes, as it was shown for the floodplain of the Ob River middle course (Krickov et al., 2021). We believe that main reasons of remarkable stability in CO_2 concentrations and emissions and weak environmental control on dissolved and

gaseous pattern in the Ket River basin are (1) essentially homogeneous landscapes, lithology and quaternary deposits of the whole river basin (20-25 % bogs, 60-70% forest, 3-5 % riparian zone), and (2) strong dominance of allochthonous sources in both dissolved and particulate organic matter. Indeed, the SUVA and bacterial number (TBC) positively correlated with both pCO_2 and FCO_2 during summer (**Fig. 5 B; Table 2**), which may indicate non-negligible role of bacterial processing of allochthonous (aromatic) DOC delivered to the water column from wetlands and mires. As such, homogeneous land cover and essentially allochthonous DOC can still lead to variations of CO_2 per stream size, with small systems showing higher values than large systems as predicted conceptually (Hotchkiss et al., 2015) and verified at basin-scale (e.g. Borges et al., 2019). Consistent with this, we observed systematically higher CO_2 concentration and flux in small tributaries [which were fed by mire waters with 'non-processed' OM] compared to the main stem (**Table 2**). Furthermore, the positive correlation between mean annual precipitation (MAP) and pCO_2 and FCO_2 during the baseflow (**Table 2, Fig. 5 D**) could reflect the importance of water storage in the mires and wetlands (which also showed positive but less significant correlations, **Table 2**) during the summer time, and progressive release of CO_2 and DOC-rich waters from the wetlands to the streams. Another indirect evidence of the mire water control on CO_2 emission from the river cmes from daily CO_2 pattern in a tributary of the Ket River (**Fig. 4 E**). For this relatively small river ($S_{watershed}$ = 472 km²), we noted that there was quite heavy rainfall, between 7 am and 3 pm, prior to the CO_2 peak which was observed at 7 pm. Given that water residence time is very short during spring flood, when the soils are partially frozen, the delivery of allochtonous DOM and elevated CO_2 from adjacent mires could be the cause of observed CO_2 peak. Generally, the terrestrial source controlling CO_2 pattern in the Ket River could be either soil litter leachates (in spring) or bog water (during baseflow, when the river water is substantially derived from wetlands, Ala-aho et al., 2018a, b). Therefore, the patterns in CO_2 emissions observed in the present study during summer baseflow thus suggest the importance of allochthonous organic matter from the peatland for CO_2 production in the water column and in soils where the degradation of DOC is enhanced by the presence of bacteria. This is consistent with observations in other regions that, during summer-time, numerous processes contribute to increase CO_2 in rivers such as higher temperature stimulating microbial metabolism, longer residence time and enhanced flow paths of soil water (Borges et al. 2018).

A correlation between CO_2 flux during baseflow and the proportion of deciduous needleleaf forest at the watershed (**Fig. 5 C**) may suggest the importance of C cycling by larch trees and their possible control on the delivery of degradable organic matter to the river. Similar control of larch vegetation on riverine CO_2 has been suggested for the Lena River, Eastern Siberia (Vorobyev et al., 2021) although we acknowledge that further observations on contrasted Siberian watersheds are necessary to confirm the observation that larch trees litterfall led to export of degradable OM to the river.

In the Ket River basin, the local soil/groundwater effects are expected to be more pronounced during baseflow, due to lower impact of dilution, compared to the spring flood period. The hypothesis of deeper flow path in summer compared to spring is confirmed for the WSL (Frey and McClelland, 2009; Pokrovsky et al., 2015; Serikova et al., 2018) and is supported in this study by a strong increase in DIC concentration between spring and summer (**Fig. 3**). Thus, although the pairwise correlations between parameters do not support any particular mechanism, it is not excluded that OM bio- and photo degradation and local mire water feeding drive FCO_2 in spring, and that deeper flowpaths and DIC export drive the elevated FCO_2 in summer. The latter is consistent with results of analysis of streams and rivers across the contiguous United States, which demonstrated that ~60% of CO_2 evasion is from external sources rather than internal production (Hotchkiss et al., 2015). In view of lack of correlation of CO_2 emissions in the Ket River and tributaries with hydrochemical parameters of the water column, we believe that external source of CO_2 in studied river system represents sizable contribution to total riverine CO_2 evasion across the seasons and sampling sites. In particular, in small peatland streams, the CO_2-rich deep peat/groundwater is known to be the major source of aquatic CO_2 under low flow conditions (Dinsmore and Billett, 2008), whereas in boreal headwater streams of N Sweden the main source of stream CO_2 was inflowing CO_2-rich soil waters (Winterdahl et al., 2016).

Another important factor responsible for higher CO_2 production in the water column in summer compared to spring could be POC degradation. The riverine POC is known to be much more biodegradable than DOC (Attermeyer et al., 2018), and the POC concentration in the Ket River basin increased 4-fold between spring and summer (**Table 1**). The origin of summer-time POC and its lability remain elusive, but could be a combination of plankton bloom and mire- or forest-derived DOC coagulation products in the water column (Krickov et al., 2018). Furthermore, pronounced heterogeneity in CO_2 emission during baseflow

among tributaries may also reflect the heterogeneity of riverine organic matter which is known to be the maximal during low flow conditions and minimal during high flow (Lynch et al., 2019).

The main unexpected result of this study is that none of the physiochemical parameters of the water column and the land cover factor is sufficiently strong to drive the CO_2 and CH_4 patterns, although they show pronounced spatial and seasonal variations. Although correlations do not necessary imply causation and some correlations could be spurious or indirect, this analysis, together with PCA treatment, allow first order assessment of possible governing factors or dismissing the environmental parameters that do not contribute in GHG pattern control. A likely explanation is that simultaneous operation of multiple aquatic processes that include carbon, oxygen, nutrient, and plankton and peryphyton dynamics as well as sediment respiration control the CO_2 and CH_4 exchanges with the atmosphere, as it is known for boreal lakes and floodplain zones of the boreal rivers (i.e., Bayer et al., 2019; Zabelina et al., 2021; Krickov et al., 2019). Given that even a multiparametric statistical treatment (PCA) did no demonstrate sizable explanation capacity of the data set, we cannot exclude that these potential physico-chemical, microbiological and landscape drivers are working in different (opposing) directions and have counteracted each other. However, further in-depth analysis of these interactions requires much better seasonal resolution, ideally over full period of the year, which was beyond the scope of the present study.

4.3. Emissions from the Ket River basin compared to downstream export of riverine carbon

The estimated C emissions (> 99.5 % C; < 0.5 % CH_4) from the Ket River main channel over 830 km distance (0.5 to 2.5 g C m^{-2} d^{-1}) are comparable to those of the Ob River main channel (1.32±0.14 g C m^{-2} d^{-1} in the permafrost-free zone; Karlsson et al., 2021). The CO_2 emission in Ket's tributaries (1 to 2 g C m^{-2} d^{-1} in spring; 1 to 5 g C m^{-2} d^{-1} in summer) are within the range reported for small rivers and streams of the permafrost-free zone of western Siberia (0 to 3.6 g C m^{-2} d^{-1} in spring; 4 to 9 g C m^{-2} d^{-1} in summer; Serikova et al., 2018), forest and wetland headwater streams of northern Sweden (0.5 to 5 g C m^{-2} d^{-1}; Gómez-Gener et al., 2021a), and boreal streams in Canada and Alaska (0.8 to 5.2 g C m^{-2} d^{-1}, Koprivnjak et al., 2010; Teodoru et al., 2009; Crawford et al., 2013; Campeau et al., 2014). Total C emissions from the water surfaces of the Ket River basin assessed in this study (148 g C-CO_2 m^{-2}_{water} y^{-1}, assuming no emission under ice), when

normalized to the Ket river basin area ($S_{watershed}$ = 94,000 km²), amounts to 1.35 g C m^{-2}_{land} y^{-1}. Generally higher land area - specific emissions, comparable or exceeding those of the Ket River, were reported in Québec (1.0 to 4.6 g C m^{-2} y^{-1}; Campeau and del Giorgio, 2014; Hutchins et al., 2019; Teodoru et al., 2009), Sweden (1.6 to 8.6 g C m^{-2} y^{-1}; Humborg et al., 2010; Jonsson et al., 2007; Lundin et al., 2013; Wallin et al., 2011, 2018) and boreal portions of the Yukon River (7 to 9 g C m^{-2} y^{-1}; Striegl et al., 2012; Stackpoole et al., 2017). Possible reasons for these differences could be different areal coverage of the territory by river network, the calculated rather than measured CO_2 fluxes, or the higher gas transfer velocity in the rivers from mountainous regions.

The regional assessment of the Ket River basin performed in this study are based on direct chamber measurements of emissions and as such provide rigorous basis for upscaling the CO_2 emissions from currently understudied lotic waters of permafrost-free zone of Western Siberia. The C evasion from the fluvial network of the Ket River assessed in the present work (127 ± 11 Gg y^{-1}, ignoring the emission during the ice breakup in early spring) is 3 times lower than the total (DOC+DIC+POC) downstream export by this river from the same territory (0.35 Tg C y^{-1}). The riverine C yield for the Ket River (3.7 t C km^{-2}_{land} y^{-1}) is in agreement with regional C (DOC+DIC) yield by permafrost-free small and medium size rivers of the WSL (3 to 4 t C km^{-2}_{land} y^{-1}, Pokrovsky et al., 2020) and with the Ob River in the permafrost-free zone (3.6 t C km^{-2}_{land} y^{-1}, Vorobyev et al., 2019). Note that the latter study of the Ob River, which is very similar in the environmental context to the Ket River, included high frequency weekly sampling over several years of monitoring. Thus, the similarity of downstream export fluxes of the Ket and Ob Rivers support the validity of approaches for sampling and C yield calculation employed in the present study. Such high C yields in the southern, permafrost-free part of the WSL stem from essentially inorganic carbon originated from groundwater discharge of carbonate mineral rich reservoirs, abundant in this region (Pokrovsky et al., 2015). At the same time, the organic C yield in rivers of this region is quite low and represents less than 20 % of total C yield (Pokrovsky et al., 2020; Vorobyev et al., 2019). This can explain anomalously low value of C evasion : C export of the Ket River (1 : 3) measured in this work as compared to the average values for permafrost-free zone of Western Siberia (1 : 1, Serikova et al., 2019). One should also note that the gas transfer velocity measured in this study provides much lower fluxes than those calculated with K_T = 4.46 m d^{-1} in previous

studies (**Table S2**). Another factor potentially leading to underestimation of C evasion in this study is GIS-based minimal water coverage which does not include seasonal oxbow lakes, flooded forest and temporary water bodies of the floodplain which provide sizable emissions (see Krickov et al., 2021). We also do not exclude that some important hot moments / hot spots of C emission were missed in our sampling campaign, such as summer baseflow/autumn peaks (Serikova et al., 2019) or stagnant zones of the floodplain in summer (Krickov et al., 2021; Castro-Morales et al., 2021). This calls a need for higher spatial and temporal resolution monitoring of C emission, with special focus on important events across full hydrological continuum.

5. Concluding remarks

Via combination of discrete floating chamber and hydrochemistry and continuous CO_2 concentration measurements over 830 km of large pristine boreal river of western Siberia main channel and its 26 tributaries during the peak of spring flood and the summer-autumn baseflow, we quantified spatial and temporal variations, overall emissions of C (CO_2, CH_4) and export of (DOC, DIC and POC) during the 6 months of open water period. The range of CO_2 and CH_4 concentrations in the main channel and tributaries as well as CO_2 emissions were consistent with other boreal and subarctic regions but demonstrated rather low seasonal and spatial variability. The diel CO_2 flux by floating chambers and continuous pCO_2 measurements in the tributaries of the Ket River during spring flood demonstrated negligible impact of day/night period on the CO_2 concentrations and emission fluxes.

We hypothesize that homogeneous landscape coverage (bog and taiga forest) provide stable allochthonous input of DOM as confirmed by very weak spatial and seasonal variations of DOM aromaticity. Among possible driving factors of CO_2 production in the water column (bio- and photo-degradation of DOC and POC, plankton metabolism), none seems to be sizably important for persistent CO_2 supersaturation and relevant emissions. The landscape factors of the watershed (bog and forest coverage, soil organic carbon stock) of the tributaries and along the main stem did not sizably affected the C concentration and emission pattern across two seasons. We hypothesize that stable terrestrial input of strongly aromatic DOM, shallow photic layer and humic waters of the Ket River basin preclude sizable daily and seasonal variations of C parameters. Punctual discharge of groundwater, resuspension of sediments or shallow subsurface influx from

mires and riparian zone may be responsible for small-scale heterogeneities in C emissions and concentrations along the main stem and among the tributaries. These effects are much stronger pronounced during summer baseflow compared to spring flood. Overall, deeper flow paths in summer compared to spring enhance the DIC discharge within the river bed and the tributaries, thus leading to elevated CO_2 flux in summer. Additional factor responsible for higher CO_2 emission during this season could be mire-originated particulate organic matter (POM) processing in the water column.

The six month open-water period C emissions from the lotic waters of the Ket River basin were sizably lower than the downstream total C export by this river during the same period. We conclude that regional estimations of C balance in lotic systems should be based on a combination of direct chamber measurements, discrete hydrochemical sampling and continuous in-situ monitoring with submersible sensors, at least during two most important hydrological periods of the year which are, for boreal regions, the spring flood and the summer-autumn baseflow. We believe that this is the best trade-off between scientific rigor and logistical feasibility in poorly accessible, pristine and strongly understudied regions.

Acknowledgements.

We acknowledge support from RSF grant 22-17-00253, RFBR grant 20-05-00729, the TSU Development Program "Priority-2030", grant "Kolmogorov" of MES (Agreement No 075-15-2022-241), and the Swedish Research Council (grant no. 2016-05275).

Authors contribution.

AL and OP designed the study and wrote the paper; AL, SV, IK and OP performed sampling, analysis and their interpretation; LS performed bacterial assessment and DOC/DIC analysis and interpretation; MK performed landscape characterization of the Ket River basin and calculated water surface area; SK performed hydrological analysis; JK provided analyses of literature data, transfer coefficients for FCO_2 calculations and global estimations of areal emission vs export.

Competing interests.

The authors declare that they have no conflict of interest.

References

Abril, G., Martinez, J.-M., Artigas, L. F., Moreira-Turcq, P., Benedetti, M. F., Vidal, L., Meziane, T., Kim, J.-H., Bernardes, M. C., Savoye, N., Deborde, J., Albéric, P., Souza, M. F. L., Souza, E. L., and Roland, F.: Amazon river carbon dioxide outgassing fueled by wetlands, Nature, 505, 395-398, https://doi.org/10.1038/nature12797, 2014.

Abril, G. and Borges, A. V.: Ideas and perspectives: Carbon leaks from flooded land: do we need to replumb the inland water active pipe? Biogeosciences, 16, 769–784, https://doi.org/10.5194/bg-16-769-2019, 2019.

Ala-Aho, P., Soulsby, C., Pokrovsky, O. S., Kirpotin, S. N., Karlsson, J., Serikova, S., Manasypov, R., Lim, A., Krickov, I., Kolesnichenko, L. G., Laudon, H., and Tetzlaff, D.: Permafrost and lakes control river isotope composition across a boreal Arctic transect in the Western Siberian lowlands, Environ. Res. Lett., 13, https://doi.org/10.1088/1748-9326/aaa4fe, 2018a.

Ala-aho, P., Soulsby, C., Pokrovsky, O. S., Kirpotin, S. N., Karlsson, J., Serikova, S., Vorobyev, S. N., Manasypov, R. M., Loiko, S., and Tetzlaff, D.: Using stable isotopes to assess surface water source dynamics and hydrological connectivity in a high-latitude wetland and permafrost influenced landscape, J. Hydrol., 556, 279–293, https://doi.org/10.1016/j.jhydrol.2017.11.024, 2018b.

Alin, S. R., Rasera, M. D. F. F. L., Salimon, C. I., Richey, J. E., Holtgrieve, G. W., Krusche, A. V., and Snidvongs, A.: Physical controls on carbon dioxide transfer velocity and flux in low-gradient river systems and implications for regional carbon budgets, J. Geophys. Res. Biogeosciences, 116, https://doi.org/10.1029/2010JG001398, 2011.

Allen, G. H. and Pavelsky, T. M.: Global extent of rivers and streams, Science, 361, 585–588, https://doi.org/10.1126/science.aat0636, 2018.

Almeida, R. M., Pacheco, F. S., Barros, N., Rosi, E., and Roland, F.: Extreme floods increase CO_2 outgassing from a large Amazonian rive, Limnol. Oceanogr., 62, 989–999, https://doi.org/10.1002/lno.10480, 2017.

Amaral, J. H. F., Borges, A. V., Melack, J. M., Sarmento, H., Barbosa, P. M., Kasper, D., Melo, M. L., de Fex Wolf., D., da Silva, J. S., and Forsberg, B. R.: Influence of plankton metabolism and mixing depth on CO_2 dynamics in an Amazon floodplain lake, Sci. Total. Env. 630, 1381-1393, https://doi.org/10.1016/j.scitotenv.2018.02.331, 2018.

Amaral, J. H. F., Melack, J. M., Barbosa, P. M., Borges, A. V., Kasper, D., Cortes, A. C., Zhou, W., MacIntyre, S., and Forsberg, B. R.: Inundation, hydrodynamics and vegetation influences carbon dioxide concentrations in Amazon floodplain lakes, Ecosystem, 25(4), 911–930, https://doi.org/10.1007/s10021-021-00692-y, 2022.

Attermeyer, K., Catalán, N., Einarsdottir, K., Freixa, A., Groeneveld, M., Hawkes, J. A., Bergquist, J., and Tranvik, L. J.: Organic carbon processing during transport through boreal inland waters: particles as important sites, J. Geophys. Res. Biogeosciences, 123, 2412–2428, https://doi.org/10.1029/2018JG004500, 2018.

Bartalev, S. A., Egorov, V. A., Ershov, D. V., Isaev, A. S., Lupyan, E. A., Plotnikov, D. E., and Uvarov, I. A.: Remote mapping of vegetation land cover of Russia based on data of MODIS spectroradmeter, Mod. Probl. Earth Remote Sens. Space, 8, 285–302, 2018.

Bastviken, D., Sundgren, I., Natchimuthu, S., Reyier, H., and Gålfalk, M.: Technical Note: Cost-efficient approaches to measure carbon dioxide (CO_2) fluxes and concentrations in terrestrial and aquatic environments using mini loggers, Biogeosciences, 12, 3849–3859, https://doi.org/10.5194/bg-12-3849-2015, 2015.

Bayer, T. K., Gustafsson, E., Brakebusch, M., and Beer, C.: Future carbon emission from boreal and permafrost lakes are sensitive to catchment organic carbon loads, J. Geophys. Res. Biogeosciences, 124, 1827-1848, https://doi.org/10.1029/2018JG004978, 2019.

Beaulieu, J. J., Shuster, W. D., and Rebholz, J. A.: Controls on gas transfer velocities in a large river, J. Geophys. Res. Biogeosciences, 117, G02007, https://doi.org/10.1029/2011JG001794, 2012.

Borges, A. V., Darchambeau, F., Lambert, T., Bouillon, S., Morana, C., Brouyère, S., Hakoun, V., Jurado, A., Tseng, H-C., Descy, J.-P., and Roland, F. A. E.: Effects of agricultural land use on fluvial carbon

dioxide, methane and nitrous oxide concentrations in a large European river, the Meuse (Belgium), Sci. Total Environ., 610-611, 342-355, https://doi.org/10.1016/j.scitotenv.2017.08.047, 2018.

Borges, A. V., Darchambeau, F., Teodoru, C. R., Marwick, T. R., Tamooh, F., Geeraert, N., Omengo, F. O., Guérin, F., Lambert, T., Morana, C., Okuku, E., and Bouillon, S.: Globally significant greenhouse gas emissions from African inland waters, Nature Geoscience, 8, 637-642, https://doi.org/10.1038/NGEO2486, 2015.

Bussmann, I.: Distribution of methane in the Lena Delta and Buor-Khaya Bay, Russia, Biogeosciences, 10, 4641–4652, https://doi.org/10.5194/bg-10-4641-2013, 2013.

Cai, W.-J. and Wang, Y.: The chemistry, fluxes, and sources of carbon dioxide in the estuarine waters of the Satilla and Altamaha Rivers, Georgia, Limnol. Oceanogr., 43, 657–668, https://doi.org/10.4319/lo.1998.43.4.0657, 1998.

Campeau, A. and del Giorgio, P. A.: Patterns in CH_4 and CO_2 concentrations across boreal rivers: Major drivers and implications for fluvial greenhouse emissions under climate change scenarios, Glob. Change Biol., 20, 1075–1088, https://doi.org/10.1111/gcb.12479, 2014.

Campeau, A., Lapierre, J.-F., Vachon, D., and del Giorgio, P. A.: Regional contribution of CO_2 and CH_4 fluxes from the fluvial network in a lowland boreal landscape of Québec, Glob. Biogeochem. Cycles, 28, 57–69, https://doi.org/10.1002/2013GB004685, 2014.

Castro-Morales, K., Canning, A., Körtzinger, A., Göckede, M., Küsel, K., Overholt, W. A., Wichard, T., Redlich, S., Arzberger, S., Kolle, O., and Zimov, N.: Effects of reversal of water flow in an Arctic floodplain river on fluvial emissions of CO_2 and CH_4, J. Geophys. Res. Biogeosciences, 127, e2021JG006485, https://doi.org/10.1029/2021JG006485, 2022.

Chadburn, S. E., Krinner, G., Porada, P., Bartsch, A., Beer, C., Belelli Marchesini, L., Boike, J., Ekici, A., Elberling, B., Friborg, T., Hugelius, G., Johansson, M., Kuhry, P., Kutzbach, L., Langer, M., Lund, M., Parmentier, F.-J. W., Peng, S., Van Huissteden, K., Wang, T., Westermann, S., Zhu, D., and Burke, E. J.: Carbon stocks and fluxes in the high latitudes: using site-level data to evaluate Earth system models, Biogeosciences, 14, 5143–5169, https://doi.org/10.5194/bg-14-5143-2017, 2017.

Cole, J. J. and Caraco, N. F.: Atmospheric exchange of carbon dioxide in a low-wind oligotrophic lake measured by the addition of SF6, Limnol. Oceanogr., 43, 647–656, https://doi.org/10.4319/lo.1998.43.4.0647, 1998.

Cooper, L. W., McClelland, J. W., Holmes, R. M., Raymond, P. A., Gibson, J. J., Guay, C. K., and Peterson, B. J.: Flow-weighted values of runoff tracers ($\delta^{18}O$, DOC, Ba, alkalinity) from the six largest Arctic rivers, Geophys. Res. Lett., 35, L18606, https://doi.org/10.1029/2008GL035007, 2008.

Crawford, J. T., Striegl, R. G., Wickland, K. P., Dornblaser, M. M., and Stanley, E. H.: Emissions of carbon dioxide and methane from a headwater stream network of interior Alaska, J. Geophys. Res. Biogeosciences, 118, 482–494, https://doi.org/10.1002/jgrg.20034, 2013.

Crawford, J. T., Loken, L. C., Casson, N. J., Smith, C., Stone, A. G., and Winslow, L. A.: High-speed limnology: using advanced sensors to investigate spatial variability in biogeochemistry and hydrology, Environ. Sci. Technol., 49, 442–450, https://doi.org/10.1021/es504773x, 2015.

Crawford, J. T., Stanley, E. H., Dornblaser, M. M., and Striegl, R. G.: CO_2 time series patterns in contrasting headwater streams of North America, Aquatic Sciences, 79, 473-486, https://doi.org/10.1007/s00027-016-0511-2, 2016a.

Crawford, J. T., Loken, L. C., Stanley, E. H., Stets, E. G., Dornblaser, M. M., and Striegl, R. G.: Basin scale controls on CO_2 and CH_4 emissions from the Upper Mississippi River, Geophys. Res. Lett., 43, 1973–1979, https://doi.org/10.1002/2015GL067599, 2016b.

Crawford, J. T., Butman, D. E., Loken, L. C., Stadler, P., Kuhn, C., and Striegl, R. G.: Spatial variability of CO_2 concentrations and biogeochemistry in the Lower Columbia River, Inland Waters, 7, 417-427, https://doi.org/10.1080/20442041.2017.1366487, 2017.

Dawson, J. J., Billett, M. F., Hope, D., Palmer, S. M., and Deacon, C.: Sources and sinks of aquatic carbon in a peatland stream continuum, Biogeochemistry, 70, 71–92, 2004.

Descy, J. P., Darchambeau, F., Lambert, T., Stoyneva, M. P., Bouillon, S., and Borges, A. V.: Phytoplankton dynamics in the Congo River, Freshwater Biology, 62, 87–101, https://doi.org/10.1111/fwb.12851, 2017.

DelDuco, E. M. and Xu, Y. J.: Dissolved carbon transport and processing in North America's largest swamp river entering the Northern Gulf of Mexico, Water, 11, 1395, https://doi.org/10.3390/w11071395, 2019.
Denfeld, B. A., Frey, K. E., Sobczak, W. V., Mann, P. J., and Holmes, R. M.: Summer CO_2 evasion from streams and rivers in the Kolyma River basin, north-east Siberia, Polar Res., 32, 19704, https://doi.org/10.3402/polar.v32i0.19704, 2013.
Dinsmore, K. J. and Billett, M. F.: Continuous measurement and modeling of CO_2 losses from a peatland stream during stormflow events, Water Resour. Res., 44, W12417, https://doi.org/10.1029/2008WR007284, 2008.
Dinsmore, K. J., Billett, M. F., and Dyson, K. E.: Temperature and precipitation drive temporal variability in aquatic carbon and GHG concentrations and fluxes in a peatland catchment, Glob. Change Biol., 19, 2133–2148, https://doi.org/10.1111/gcb.12209, 2013.
Elder, C. D., and others.: Greenhouse gas emissions from diverse Arctic Alaskan lakes are dominated by young carbon, Nature Climate Change 8, 166-171, doi: 10.1038/s41558-017-0066-9, 2018.
Feng, X., Vonk, J. E., Dongen, B. E. V., Gustafsson, Ö., Semiletov, I. P., Dudarev, O. V., Wang, Z., Montluçon, D. B., Wacker, L., and Eglinton, T. I.: Differential mobilization of terrestrial carbon pools in Eurasian Arctic river basins, Proc. Natl. Acad. Sci. U. S. A., 110, 14168–14173, https://doi.org/10.1073/pnas.1307031110, 2013.
Foster-Martinez, M. R. and Variano, E. A.: Air-water gas exchange by waving vegetation stems, J. Geophys. Res. Biogeosciences, 121, 1916–1923, https://doi.org/10.1002/2016JG003366, 2016.
Frey, K. E. and Smith, L. C.: How well do we know northern land cover? Comparison of four global vegetation and wetland products with a new ground-truth database for West Siberia. Glob. Biogeochem. Cycles, 21, GB1016. https://doi.org/10.1029/2006GB002706, 2007.
Frey, K. E. and McClelland, J. W.: Impacts of permafrost degradation on arctic river biogeochemistry, Hydrol. Process., 23, 169–182, https://doi.org/10.1002/hyp.7196, 2009.
Gómez-Gener, L., Rocher-Ros, G., Battin, T., Cohen, M. J., Dalmagro, H. J., Dinsmore, K. J., Drake, T. W., Duvert, C., Enrich-Prast, A., Horgby, Å., Johnson, M. S., Kirk, L., Machado-Silva, F., Marzolf, N. S., McDowell, M. J., McDowell, W. H., Miettinen, H., Ojala, A. K., Peter, H., Pumpanen, J., Ran, L., Riveros-Iregui, D. A., Santos, I. R., Six, J., Stanley, E. H., Wallin, M. B., White, S. A., and Sponseller, R. A.: Global carbon dioxide efflux from rivers enhanced by high nocturnal emissions, Nat. Geosci., 1–6, https://doi.org/10.1038/s41561-021-00722-3, 2021a.
Gómez-Gener, L., Hotchkiss, E. R., Laudon, H., and Sponseller, R. A.: Integrating discharge-concentration dynamics across carbon forms in a boreal landscape, Water Resour. Res., 57, e2020WR028806, https://doi.org/10.1029/2020WR028806, 2021b.
Griffin, C. G., McClelland, J. W., Frey, K. E., Fiske, G., and Holmes, R. M.: Quantifying CDOM and DOC in major Arctic rivers during ice-free conditions using Landsat TM and ETM+ data, Remote Sens. Environ., 209, 395–409, https://doi.org/10.1016/j.rse.2018.02.060, 2018.
Guérin, F., Abril, G., Serça, D., Delon, C., Richard, S., Delmas, R., Tremblay, A., and Varfalvy, L.: Gas transfer velocities of CO_2 and CH_4 in a tropical reservoir and its river downstream, J. Mar. Syst., 66, 161–172, https://doi.org/10.1016/j.jmarsys.2006.03.019, 2007.
Harris, I., Jones, P. d., Osborn, T. j., and Lister, D. h.: Updated high-resolution grids of monthly climatic observations – the CRU TS3.10 Dataset, Int. J. Climatol., 34, 623–642, https://doi.org/10.1002/joc.3711, 2014.
Ho, D. T., Engel, V. C., Ferrón, S., Hickman, B., Choi, J., and Harvey, J. W.: On factors influencing air-water gas exchange in emergent wetlands, J. Geophys. Res. Biogeosciences, 123, 178–192, https://doi.org/10.1002/2017JG004299, 2018.
Holmes, R. M., McClelland, J. W., Peterson, B.J ., & Tank S. E. et al. Seasonal and annual fluxes of nutrients and organic matter from large rivers to the Arctic Ocean and surrounding seas, Estuaries and Coasts, 35, 369-382. doi: 10.1007/s12237-011-9386-6, 2012.
Holmes, R. M., Coe, M. T., Fiske, G. J., Gurtovaya, T., McClelland, J. W., Shiklomanov, A. I., Spencer, R. G. M., Tank, S. E., and Zhulidov, A. V.: Climate change impacts on the hydrology and biogeochemistry of Arctic Rivers, in: Climatic Changes and Global warming of Inland Waters: Impacts and Mitigation for Ecosystems and Societies, edited by: Goldman, C. R., Kumagi, M., and Robarts, R. D., John Wiley and Sons, 1–26, 2013.

Hotchkiss, E. R., Hall Jr, R. O., Sponseller, R. A., Butman, D., Klaminder, J., Laudon, H., Rosvall, M., and Karlsson, J.: Sources of and processes controlling CO_2 emissions change with the size of streams and rivers, Nat. Geosci., 8, 696–699, https://doi.org/10.1038/ngeo2507, 2015.

Hugelius, G., Tarnocai, C., Broll, G., Canadell, J. G., Kuhry, P., and Swanson, D. K.: The northern circumpolar soil carbon database: Spatially distributed datasets of soil coverage and soil carbon storage in the northern permafrost regions, Earth Syst. Sci. Data, 5, 3–13, https://doi.org/10.5194/essd-5-3-2013, 2013.

Humborg, C., Mörth, C.-M., Sundbom, M., Borg, H., Blenckner, T., Giesler, R., and Ittekkot, V.: CO_2 supersaturation along the aquatic conduit in Swedish watersheds as constrained by terrestrial respiration, aquatic respiration and weathering, Glob. Change Biol., 16, 1966–1978, https://doi.org/10.1111/j.1365-2486.2009.02092.x, 2010.

Hutchins, R. H. S., Prairie, Y. T., and del Giorgio, P. A.: Large-Scale Landscape Drivers of CO_2, CH_4, DOC, and DIC in Boreal River Networks, Glob. Biogeochem. Cycles, 33, 125–142, https://doi.org/10.1029/2018GB006106, 2019.

Hutchins, R. H. S., Tank, S. E., Olefeldt, D., Quinton, W. L., Spence, C., Dion, N., Estop-Aragonés, C., and Mengistu, S. G.: Fluvial CO_2 and CH_4 patterns across wildfire-disturbed ecozones of subarctic Canada: Current status and implications for future change, Glob. Change Biol., 26, 2304–2319, https://doi.org/10.1111/gcb.14960, 2020.

Johnson, M. S., Billett, M. F., Dinsmore, K. J., Wallin, M., Dyson, K. E., and Jassal, R. S.: Direct and continuous measurement of dissolved carbon dioxide in freshwater aquatic systems—method and applications, Ecohydrology, 3, 68–78, https://doi.org/10.1002/eco.95, 2009.

Jonsson, A., Algesten, G., Bergström, A.-K., Bishop, K., Sobek, S., Tranvik, L. J., and Jansson, M.: Integrating aquatic carbon fluxes in a boreal catchment carbon budget, J. Hydrol., 334, 141–150, https://doi.org/10.1016/j.jhydrol.2006.10.003, 2007.

Karlsson, J., Serikova, S., Vorobyev, S. N., Rocher-Ros, G., Denfeld, B., and Pokrovsky, O. S.: Carbon emission from Western Siberian inland waters, Nat. Commun., 12, 825, https://doi.org/10.1038/s41467-021-21054-1, 2021.

Kokic, J., Wallin, M. B., Chmiel, H. E., Denfeld, B. A., and Sobek, S.: Carbon dioxide evasion from headwater systems strongly contributes to the total export of carbon from a small boreal lake catchment, J. Geophys. Res. Biogeosciences, 120, 13–28, https://doi.org/10.1002/2014JG002706, 2015.

Koprivnjak, J.-F., Dillon, P. J., and Molot, L. A.: Importance of CO_2 evasion from small boreal streams, Glob. Biogeochem. Cycles, 24, GB4003, https://doi.org/10.1029/2009GB003723, 2010.

Krickov, I. V., Lim, A. G., Manasypov, R. M., Loiko, S. V., Shirokova, L. S., Kirpotin, S. N., Karlsson, J., and Pokrovsky, O. S.: Riverine particulate C and N generated at the permafrost thaw front: Case study of western Siberian rivers across a 1700 km latitudinal transect, Biogeosciences, 6867–6884, https://doi.org/10.5194/bg-15-6867-2018, 2018.

Krickov, I. V., Serikova, S., Pokrovsky, O. S., Vorobyev, S. N., Lim, A. G., Siewert, M. B., and Karlsson, J.: Sizable carbon emission from the floodplain of Ob River, Ecol. Indic., 131, 108164, https://doi.org/10.1016/j.ecolind.2021.108164, 2021.

Lauerwald, R., Laruelle, G. G., Hartmann, J., Ciais, P., and Regnier, P. A. G.: Spatial patterns in CO2 evasion from the global river network, Glob. Biogeochem. Cycles, 29, 534–554, https://doi.org/10.1002/2014GB004941, 2015.

Laurion, I., Vincent, W. F., MacIntyre, S., Retamal, L., Dupont, C., Francus, P., and Pienitz, R.: Variability in greenhouse gas emissions from permafrost thaw ponds, Limnol. Oceanogr., 55, 115-133, https://doi.org/10.4319/lo.2010.55.1.0115, 2010.

Leith, F. I., Dinsmore, K. J., Wallin, M. B., Billett, M. F., Heal, K. V., Laudon, H., Öquist, M. G., and Bishop, K.: Carbon dioxide transport across the hillslope–riparian–stream continuum in a boreal headwater catchment, Biogeosciences, 12, 1881–1892, https://doi.org/10.5194/bg-12-1881-2015, 2015.

Leng, P., Li, Z., Zhang, Q., Li, F., and Koschorreck, M.: Fluvial CO_2 and CH_4 in a lowland agriculturally impacted river network: Importance of local and longitudinal controls, Environ. Pollution 303, Art No 119125, https://doi.org/10.1016/j.envpol.2022.119125, 2022.

Li, M., Peng, C., Zhang, K., Xu, L., Wang, J., Yang, Y., Li, P., Liu, Z., and He, N.: Headwater stream ecosystem: an important source of greenhouse gases to the atmosphere, Water Res., 190, 116738, https://doi.org/10.1016/j.watres.2020.116738, 2021.

Liss, P. S., and Slater, P. G.: Flux of gases across the air-sea interface, Nature 247, 181–184, 1974.

Liu S., Kuhn, C., Amatulli, G., Aho, K., Butman, D.E., Allen, G.H., Lin, P., Pan, M., Yamazaki, D., Brinkerhoff, C., Gleason, C., Xia, X., and Raymond, P.A.: The importance of hydrology in routing terrestrialcarbon to the atmosphere via global streams and rivers, PNAS 119 No. 11, e2106322119; https://doi.org/10.1073/pnas.2106322119, 2022.

Lobbes, J. M., Fitznar, H. P., and Kattner, G.: Biogeochemical characteristics of dissolved and particulate organic matter in Russian rivers entering the Arctic Ocean, Geochim. Cosmochim. Acta, 64, 2973–2983, https://doi.org/10.1016/S0016-7037(00)00409-9, 2000.

Lorke A., Bodmer, P., Noss, C., Alshboul, Z., Koschorreck, M., Somlai-Haase, C., Bastviken, D., Flury, S., McGinnis, D.F., Maeck, A., Müller, D., and Premke, K.: Technical note: drifting versus anchored flux chambers for measuring greenhouse gas emissions from running waters, Biogeosciences, 12, 7013–7024, https://doi.org/10.5194/bg-12-7013-2015, 2015.

Lundin, E. J., Giesler, R., Persson, A., Thompson, M. S., and Karlsson, J.: Integrating carbon emissions from lakes and streams in a subarctic catchment, J. Geophys. Res. Biogeosciences, 118, 1200–1207, https://doi.org/10.1002/jgrg.20092, 2013.

Lynch, L. M., Sutfin, N. A., Fegel, T. S., Boot, C. M., Covino, T. P., and Wallenstein, M. D.: River channel connectivity shifts metabolite composition and dissolved organic matter chemistry, Nat. Commun., 10, 459, https://doi.org/10.1038/s41467-019-08406-8, 2019.

Marie, D., Partensky, F., Vaulot, D., and Brussaard, C.: Enumeration of Phytoplankton, Bacteria, and Viruses in Marine Samples, Curr. Protoc. Cytom., 10, 11111–111115, https://doi.org/10.1002/0471142956.cy1111s10, 1999.

Pangala, S., Enrich-Prast, A., Basso, L., Peixoto, R. B., Bastviken, D., Hornibrook, E. R. C., Gatti, L. V., Ribeiro, H., et al.: Large emissions from floodplain trees close the Amazon methane budget, Nature 552, 230–234, https://doi.org/10.1038/nature24639, 2017.

Pekel, J.-F., Cottam, A., Gorelick, N., and Belward, A. S.: High-resolution mapping of global surface water and its long-term changes, Nature, 540, 418–422, https://doi.org/10.1038/nature20584, 2016.

Pokrovsky, O. S., Manasypov, R. M., Loiko, S., Shirokova, L. S., Krickov, I. A., Pokrovsky, B. G., Kolesnichenko, L. G., Kopysov, S. G., Zemtzov, V. A., Kulizhsky, S. P., Vorobyev, S. N., and Kirpotin, S. N.: Permafrost coverage, watershed area and season control of dissolved carbon and major elements in western Siberian rivers, Biogeosciences, 12, 6301–6320, https://doi.org/10.5194/bg-12-6301-2015, 2015.

Pokrovsky, O. S., Manasypov, R. M., Kopysov, S. G., Krickov, I. V., Shirokova, L. S., Loiko, S. V., Lim, A. G., Kolesnichenko, L. G., Vorobyev, S. N., and Kirpotin, S. N.: Impact of permafrost thaw and climate warming on riverine export fluxes of carbon, nutrients and metals in Western Siberia, Water (MDPI), 12, 1817, https://doi.org/10.3390/w12061817, 2020.

Pokrovsky, O. S., Manasypov, R. M., Chupakov, A. V., and Kopysov, S.: Element transport in the Taz River, western Siberia, Chemical Geology, in press, 2022.

Ran, L., Lu, X. X., Richey, J. E., Sun, H., Han, J., Yu, R., Liao, S., and Yi, Q.: Long-term spatial and temporal variation of CO_2 partial pressure in the Yellow River, China, Biogeosciences, 12, 921–932, https://doi.org/10.5194/bg-12-921-2015, 2015.

Ran, L., Lu, X. X., and Liu, S.: Dynamics of riverine CO_2 in the Yangtze River fluvial network and their implications for carbon evasion, Biogeosciences, 14, 2183–2198, https://doi.org/10.5194/bg-14-2183-2017, 2017.

Raymond, P. A., McClelland, J. W., Holmes, R. M., Zhulidov, A. V., Mull, K., Peterson, B. J., Striegl, R. G., Aiken, G. R., and Gurtovaya, T. Y.: Flux and age of dissolved organic carbon exported to the Arctic Ocean: A carbon isotopic study of the five largest arctic rivers, Glob. Biogeochem. Cycles, 21, GB4011, https://doi.org/10.1029/2007GB002934, 2007.

Raymond, P. A., Hartmann, J., Lauerwald, R., Sobek, S., McDonald, C., Hoover, M., Butman, D., Striegl, R., Mayorga, E., Humborg, C., Kortelainen, P., Dürr, H., Meybeck, M., Ciais, P., and Guth, P.: Global

carbon dioxide emissions from inland waters, Nature, 503, 355–359, https://doi.org/10.1038/nature12760, 2013.
Repo, M. E., Huttunen, J. T., Naumov, A. V., Chichulin, A. V., Lapshina, E. D., Bleuten, W., and Martikainen, P. J.: Release of CO_2 and CH_4 from small wetland lakes in western Siberia, Tellus Ser. B, Chem. Phys. Meteorol., 59, 788–796. doi: 10.1111/j.1600-0889.2007.00301.x, 2007.
Rocher-Ros, G., Sponseller, R. A., Lidberg, W., Mörth, C.-M., and Giesler, R.: Landscape process domains drive patterns of CO_2 evasion from river networks, Limnol. Oceanogr. Lett., 4, 87–95, https://doi.org/10.1002/lol2.10108, 2019.
Santoro, M., Beer, C., Cartus, O., Schmullius, C., Shvidenko, A., McCallum, I., Wegmüller, U., and Wiesmann, A.: The BIOMASAR algorithm: An approach for retrieval of forest growing stock volume using stacks of multi-temporal SAR data, in: Proceedings of ESA Living Planet Symposium, Bergen, Norway, 28 June – 2 July, 2010.
Schneider, C. L., Herrera, M., Raisle, M. L., Suarez, E., and Riveros-Iregui, D. A.: Carbon Dioxide (CO_2) Fluxes from terrestrial and aquatic environments in a high altitude tropical catchment. J Geophys. Res. Biogeosciences 125, e2020JG005844. https://doi.org/10.1029/2020JG005844, 2020.
Semiletov, I. P., Pipko, I. I., Shakhova, N. E., Dudarev, O. V., Pugach, S. P., Charkin, A. N., McRoy, C. P., Kosmach, D., and Gustafsson, Ö.: Carbon transport by the Lena River from its headwaters to the Arctic Ocean, with emphasis on fluvial input of terrestrial particulate organic carbon vs. carbon transport by coastal erosion, Biogeosciences, 8, 2407–2426, https://doi.org/10.5194/bg-8-2407-2011, 2011.
Serikova, S., Pokrovsky, O. S., Ala-Aho, P., Kazantsev, V., Kirpotin, S. N., Kopysov, S. G., Krickov, I. V., Laudon, H., Manasypov, R. M., Shirokova, L. S., Soulsby, C., Tetzlaff, D., and Karlsson, J.: High riverine CO_2 emissions at the permafrost boundary of Western Siberia, Nat. Geosci., 11, 825–829, https://doi.org/10.1038/s41561-018-0218-1, 2018.
Serikova, S., Pokrovsky, O. S., Laudon, H., Krickov, I. V., Lim, A. G., Manasypov, R. M., and Karlsson, J.: High carbon emissions from thermokarst lakes of Western Siberia, Nat. Commun., 10, https://doi.org/10.1038/s41467-019-09592-1, 2019.
Stackpoole, S. M., Butman, D. E., Clow, D. W., Verdin, K. L., Gaglioti, B. V., Genet, H., and Striegl, R. G.: Inland waters and their role in the carbon cycle of Alaska, Ecol. Appl., 27, 1403–1420, https://doi.org/10.1002/eap.1552, 2017.
Striegl, R. G., Dornblaser, M. M., McDonald, C. P., Rover, J. A., and Stets, E. G.: Carbon dioxide and methane emissions from the Yukon River system, Glob. Biogeochem. Cycles, 26, GB0E05, https://doi.org/10.1029/2012GB004306, 2012.
Teodoru, C. R., del Giorgio, P. A., Prairie, Y. T., and Camire, M.: Patterns in pCO_2 in boreal streams and rivers of northern Quebec, Canada, Glob. Biogeochem. Cycles, 23, GB2012, https://doi.org/10.1029/2008GB003404, 2009.
Tranvik, L., Cole, J. J., and Prairie, Y. T.: The study of carbon in inland waters-from isolated ecosystems to players in the global carbon cycle, Limnol. Oceanogr. Lett., 3, 41–48, https://doi.org/10.1002/lol2.10068, 2018.
Turetsky, M.R., Abbott, B.W., Jones, M.C., Anthony, K.W., Olefeldt, D., Schuur, E.A.G., Grosse, G., Kuhry, P., Hugelius, G., Koven, C., et al. : Carbon release through abrupt permafrost thaw, Nat. Geoscience, 13, 138–143, doi:10.1038/s41561-019-0526-0, 2020.
Vachon, D., Sponseller, R. A., and Karlsson, J.: Integrating carbon emission, accumulation and transport in inland waters to understand their role in the global carbon cycle, Glob. Change Biol., 27, 719–727, https://doi.org/10.1111/gcb.15448, 2021.
Vorobyev, S. N., Pokrovsky, O. S., Kolesnichenko, L. G., Manasypov, R. M., Shirokova, L. S., Karlsson, J., and Kirpotin, S. N.: Biogeochemistry of dissolved carbon, major, and trace elements during spring flood periods on the Ob River, Hydrol. Process., 33, 1579–1594, https://doi.org/10.1002/hyp.13424, 2019.
Vorobyev, S. N., Karlsson, J., Kolesnichenko, Y. Y., Korets, M. A., and Pokrovsky, O. S.: Fluvial carbon dioxide emission from the Lena River basin during the spring flood, Biogeosciences, 18, 4919–4936, https://doi.org/10.5194/bg-18-4919-2021, 2021.
Wallin, M. B., Öquist, M. G., Buffam, I., Billett, M. F., Nisell, J., and Bishop, K. H.: Spatiotemporal variability of the gas transfer coefficient (KCO_2) in boreal streams: Implications for large scale

estimates of CO_2 evasion, Glob. Biogeochem. Cycles, 25, GB3025, https://doi.org/10.1029/2010GB003975, 2011.
Wallin, M. B., Grabs, T., Buffam, I., Laudon, H., Ågren, A., Öquist, M. G., and Bishop, K.: Evasion of CO_2 from streams – The dominant component of the carbon export through the aquatic conduit in a boreal landscape, Glob. Change Biol., 19, 785–797, https://doi.org/10.1111/gcb.12083, 2013.
Wallin, M. B., Campeau, A., Audet, J., Bastviken, D., Bishop, K., Kokic, J., Laudon, H., Lundin, E., Löfgren, S., Natchimuthu, S., Sobek, S., Teutschbein, C., Weyhenmeyer, G. A., and Grabs, T.: Carbon dioxide and methane emissions of Swedish low-order streams—a national estimate and lessons learnt from more than a decade of observations, Limnol. Oceanogr. Lett., 3, 156–167, https://doi.org/10.1002/lol2.10061, 2018.
Wanninkhof, R.: Relationship between wind speed and gas exchange over the ocean, J. Geophys. Res. Oceans, 97, 7373–7382, https://doi.org/10.1029/92JC00188, 1992.
Wild, B., Andersson, A., Bröder, L., Vonk, J., Hugelius, G., McClelland, J. W., Song, W., Raymond, P. A., and Gustafsson, Ö.: Rivers across the Siberian Arctic unearth the patterns of carbon release from thawing permafrost, PNAS, 116, 10280–10285, https://doi.org/10.1073/pnas.1811797116, 2019.
Winterdahl, M., Wallin, M. B., Karlsen, R. H., Laudon, H., Öquist, M., and Lyon, S. W.: Decoupling of carbon dioxide and dissolved organic carbon in boreal headwater streams, J. Geophys. Res. Biogeosciences, 121, 2630–2651, https://doi.org/10.1002/2016JG003420, 2016.
Yamamoto, S., Alcauskas, J. B., and Crozier, T. E.: Solubility of methane in distilled water and seawater. J. Chem. Eng. Data. 21, 78–80, 1976.
Zabelina, S. V., Shirokova, L. S., Klimov, S I., Chupakov, A. V., Lim, A. G., Polishchuk, Y. M., Polishchuk, V. M., Bogdanov, A. N., Muratov, I. N., Gueren, F., Karlsson, J., and Pokrovsky, O. S.: Seasonal and spatial variations of CO2 and CH4 concentrations and fluxes in surface waters of frozen peatlands (NE Europe): morphological and hydrochemical control, Limnology Oceanography, 66 (S1), S216-S230, doi: 10.1002/lno.11560, 2021.
Zolkos, S., Tank, S. E., Striegl, R. G., and Kokelj, S. V.: Thermokarst effects on carbon dioxide and methane fluxes in streams on the Peel Plateau (NWT, Canada), J. Geophys. Res. Biogeosciences, 124, 1781–1798, https://doi.org/10.1029/2019JG005038, 2019.

Table 1. Measured hydrochemical and GHG exchange parameters in the Ket River main stem and tributaries (average ± s.d.; (*n*) is number of measurements).

		Tributaries		Main stem	
Parameter	**unit**	**Flood (*n*=26)**	**Base flow (*n*=12)**	**Flood (*n*=7)**	**Base flow (*n*=6)**
Water temperature	°C	9.48±2.25	14.9±1.24	9.06±1.59	16.5±0.54
pH		6.31±0.45	6.71±0.57	6.2±0.43	7.29±0.26
Dissolved O_2	mg L^{-1}	8.53±1.26	8.02±1.13	8.85±0.83	8.78±0.18
Specific Conductivity	µS cm^{-1}	40.7±22.7	126.9±62.1	39±14.9	181±36.8
DIC	mg L^{-1}	2.83±2.58	17.8±10.4	2.43±1.49	20.5±5.22
DOC	mg L^{-1}	21.7±3.94	15.7±7.04	21.9±4.28	16.6±3.57
$SUVA_{254}$	L mg C^{-1} m^{-1}	4.34±0.33	4.9±0.66	4.29±0.18	4.26±0.52
PON	mg L^{-1}	0.08±0.06	0.64±0.27	0.1±0.07	0.96±0.22
POC	mg L^{-1}	2.41±1.17	8±2.36	2.55±1.2	9.49±1.98
TBC	$*10^5$ cells ml^{-1}	5.89±3.26	8.69±3.21	5.95±2.83	4.94±2.15
K_T	m d^{-1}	0.53±0.38	1.21±0.52	0.77±0.55	1.22±0.37
FCO_2	g C m^{-2} d^{-1}	1.3±0.76	2.63±2.15	1.35±1.08	1.16±0.5
pCO_2	µatm	2880±680	4000±1500	2400±330	2520±980
FCH_4	mmol C m^{-2} d^{-1}	0.39±0.95	1.38±1.21	0.06±0.05	0.95±0.88
CH_4	µmol L^{-1}	0.65±0.66	1.17±0.81	0.17±0.01	0.86±0.91

Table 2. Pearson correlation coefficients of measured FCO_2, CO_2, and CH_4 concentration with hydrochemical parameters of the water column (DOC, SUVA, particulate organic carbon and nitrogen, total bacterial cells) and landscape parameters of the tributaries and the main stem of the Ket River. Significant ($p < 0.05$) values are labeled by asterisk.

	all seasons			flood			baseflow		
	CH_4	CO_2	FCO_2	CH_4	CO_2	FCO_2	CH_4	CO_2	FCO_2
Hydrochemical parameters									
pH	0.2	-0.1	-0.2	-0.1	0.1	-0.2	0.0	-0.6*	-0.6*
Dissolved O_2	-0.1	-0.7*	-0.1	0.0	-0.8*	0.1	-0.2	-0.8*	-0.7*
Specific conductivity	0.3	0.0	0.1	-0.2	0.0	0.1	0.2	-0.3	-0.6*
DIC	0.3	0.0	0.0	-0.1	0.0	0.1	0.2	-0.4	-0.7*
DOC	-0.1	0.0	0.1	0.3	0.0	-0.1	-0.2	-0.1	0.2
$SUVA_{254}$	0.1	0.2	0.3	0.4	-0.3	0.1	-0.2	0.5*	0.6*
PON	0.1	-0.1	0.2	-0.2	-0.4*	0.2	-0.4	-0.5*	-0.5
POC	0.1	-0.1	0.2	-0.2	-0.4*	0.1	-0.3	-0.3	0.1
TBC	0.2	0.2	0.1	0.3	-0.2	-0.1	0.0	0.5*	0.5*
Climatic characteristics									
MAAT	0.2	0.0	-0.5*	0.1	0.0	-0.4*	0.2	0.1	-0.5
MAP	0.0	0.3*	0.5*	0.1	0.0	0.3	0.1	0.6*	0.7*
Land-cover characteristics									
Watershed area	-0.3	-0.3*	0.2	-0.4	-0.5*	0.0	-0.2	-0.1	0.5
Dark Needleleaf Forest	0.1	0.0	-0.3	0.1	0.0	-0.3	0.2	-0.1	-0.2
Light Needleleaf Forest	0.3*	0.4*	0.2	0.4	0.2	0.0	0.4	0.7*	0.6*
Broadleaf Forest	-0.3	-0.4*	0.1	-0.5*	-0.4	0.1	-0.3	-0.6*	-0.2
Mixed Forest	0.0	-0.2	-0.3	0.1	-0.1	-0.3	-0.1	-0.4	-0.4
Peatlands and bogs	0.0	0.2	0.3	-0.1	0.0	0.2	0.1	0.2	0.4
Riparian Vegetation	-0.1	0.0	-0.1	-0.2	0.1	0.0	-0.2	-0.2	-0.5
Grassland	0.1	-0.1	0.0	-0.1	-0.2	0.1	0.3	0.0	-0.5
Recent Burns	-0.1	-0.1	0.2	-0.1	-0.2	0.1	-0.3	0.1	0.4
Water Bodies	-0.2	-0.1	0.3	-0.3	-0.3	0.2	-0.2	-0.1	0.3
Lithology characteristics									
Upper Cretaceous, Maastrichtian – (sedimentary, silicate) Lower Paleocene (sedimentary silicate rocks)	0.1	-0.4*	0.0	0.3	-0.3	0.2	0.0	-0.5*	-0.4
Paleogene. Upper Oligocene (clays and silts)	0.1	-0.2	0.1	0.1	-0.1	0.2	0.0	-0.5*	-0.2
Cretaceous.Coniacian – Campanian (carbonates)	-0.2	-0.4*	-0.3	-0.2	-0.2	-0.2	-0.3	-0.7*	-0.6*
Cretaceous.Cenoman – Turon (clays, some carbonates)	-0.2	-0.5*	-0.3	-0.3	-0.3	-0.2	-0.3	-0.7*	-0.6*

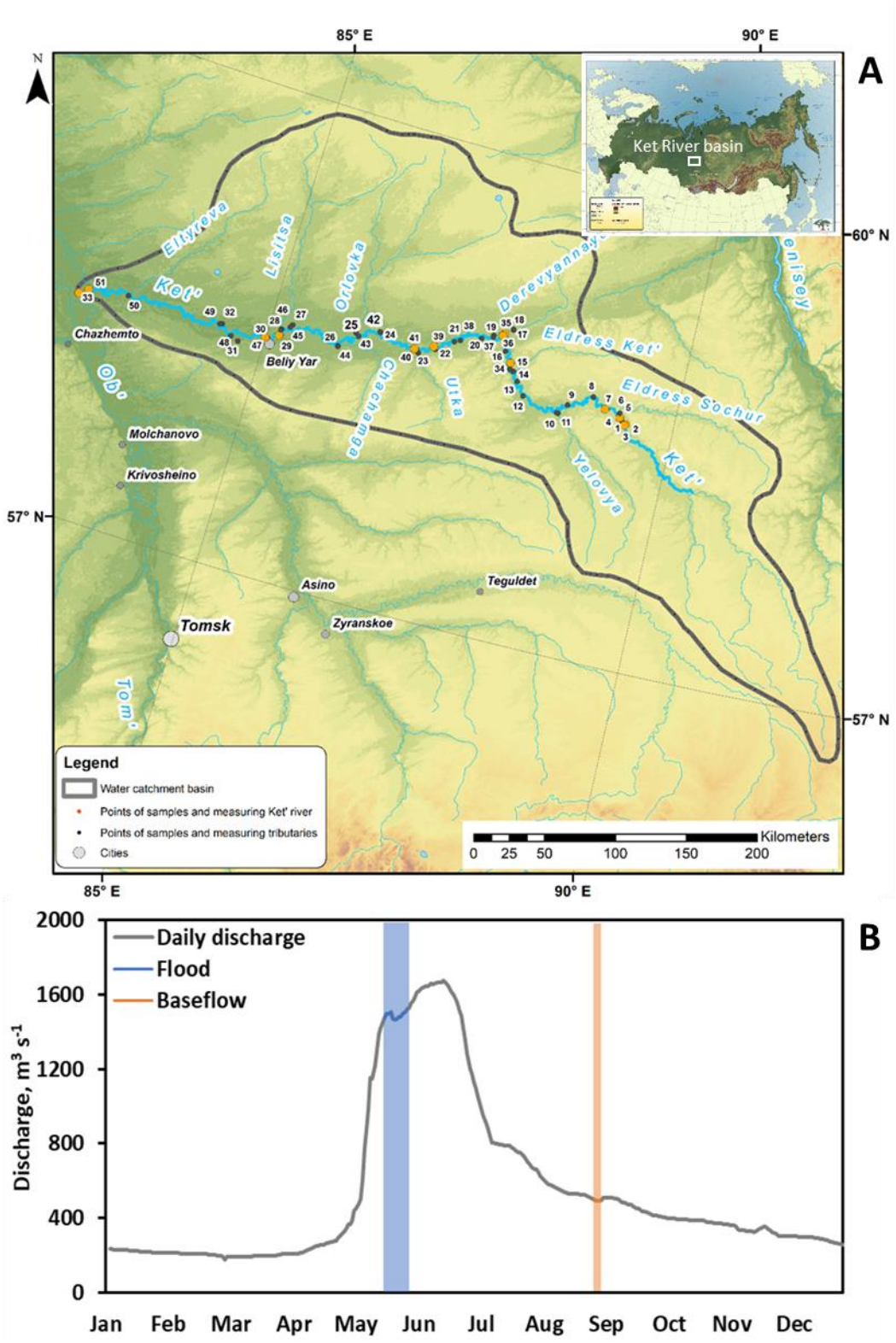

Fig. 1. A: Map of the studied Ket River watershed with continuous pCO_2 measurements in the main stem. **B:** Daily discharge (Q) at the gauging station of the Ket mouth, Rodionovka, in 2019. Highlighted in blue and orange are two sampling campaigns of this study, spring flood and summer-autumn baseflow.

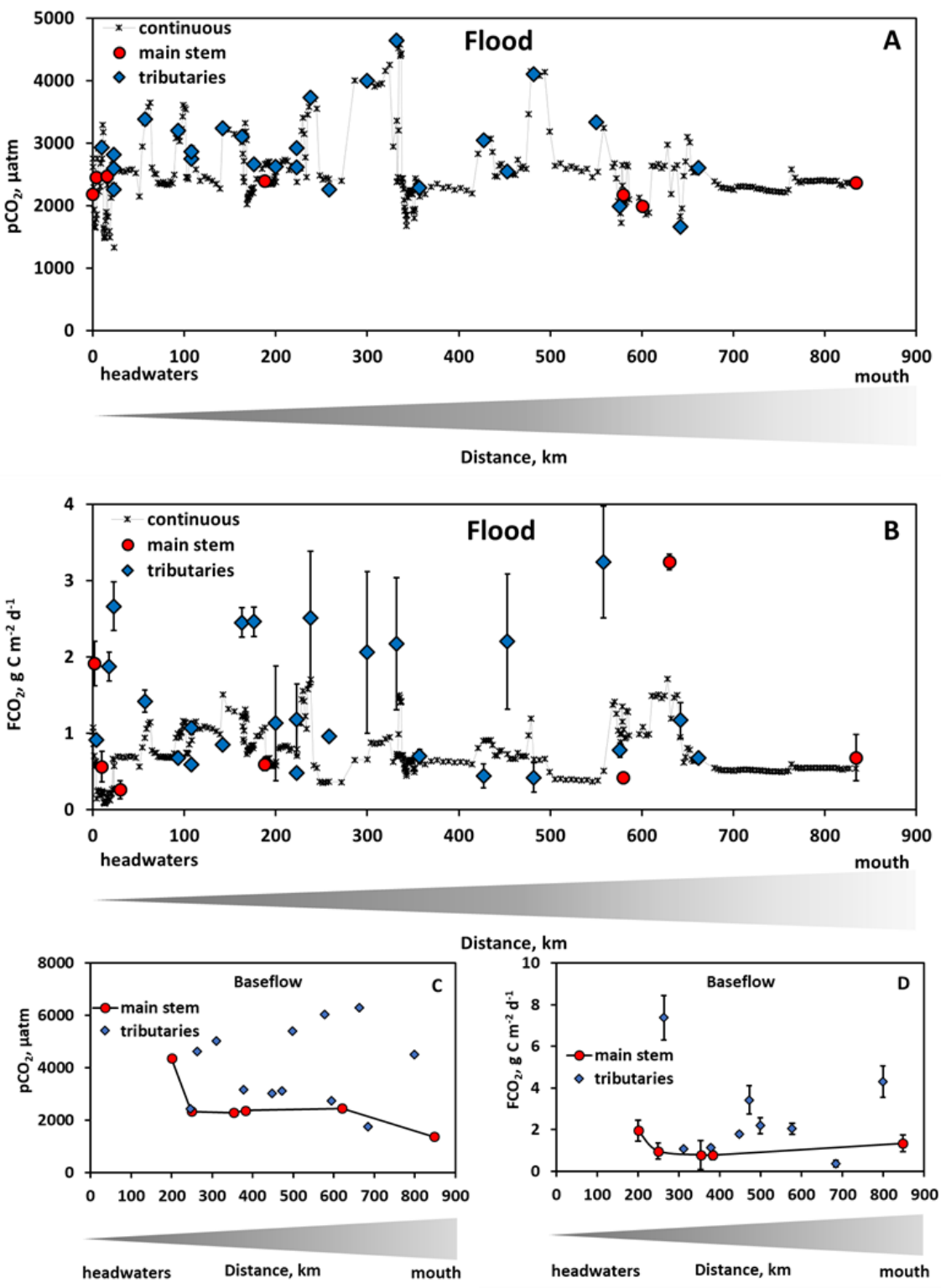

Figure 2. The measured pCO_2 (**A, C**) and CO_2 fluxes (**B, D**) during spring flood (**A, B**) and summer baseflow (**C, D**) of the Ket River main stem and tributaries (over the 830 km distance, from the headwaters to the mouth (left to right). The symbols represent discrete in situ pCO_2 (Vaissala) and FCO_2 (floating chambers) measurements of the main stem (red circles) and tributaries (blue diamonds). Continuous in-situ pCO_2 measurements and calculated FCO_2 are available only for the main stem in spring (black crosses). For the latter, we used an average value of gas transfer velocity (k_T) between two chamber sites (separated by a distance of 50 to 100 km) to calculate the FCO_2 from in-situ measured pCO_2 in the river section between these two sites. Note that during summer baseflow, the water level did not allow reaching the headwaters of the Ket River (first 0-200 km on the river course).

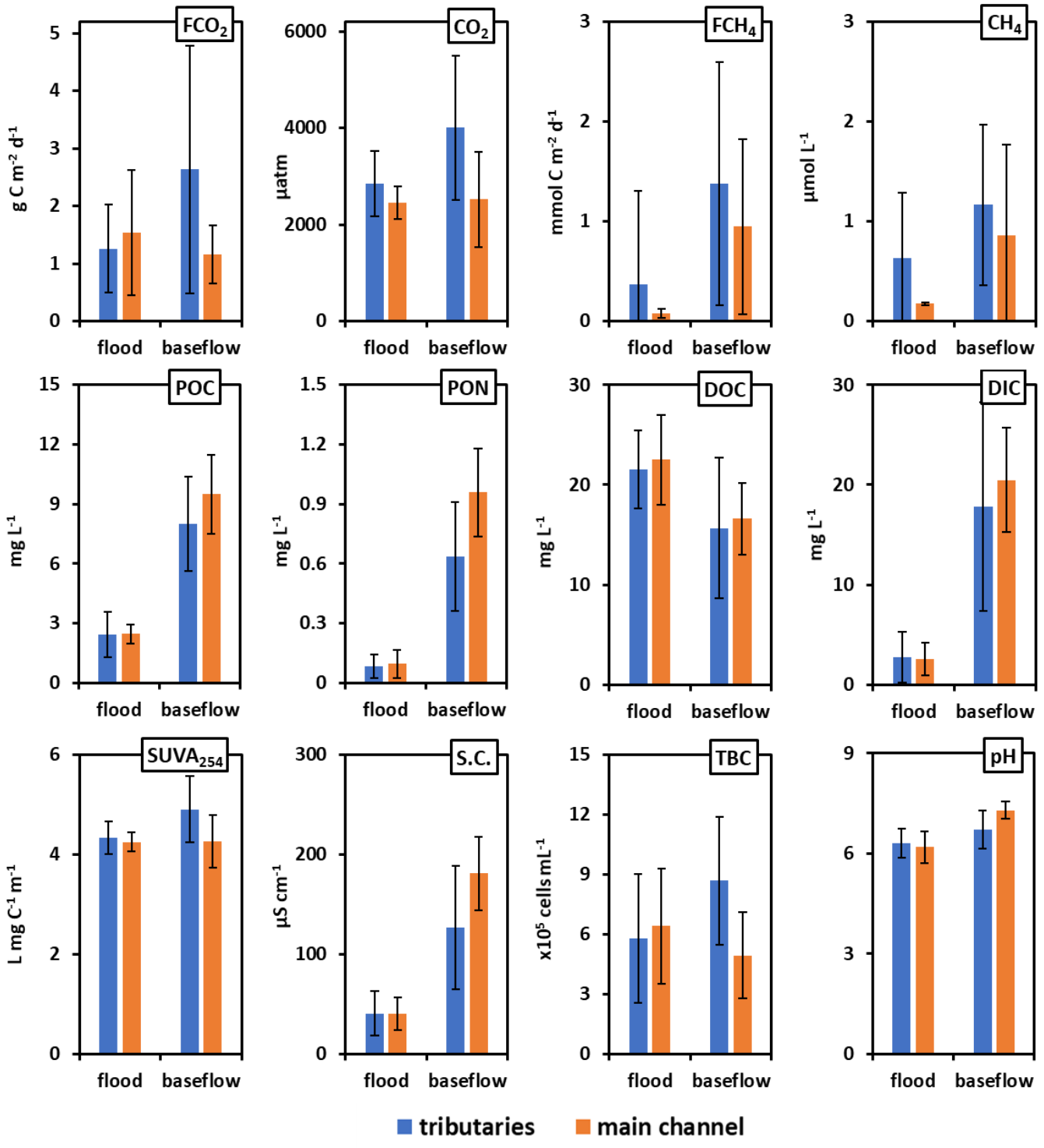

Figure 3. Mean (± s.d.) GHG concentration and fluxes, hydrochemical parameters, particulate organic carbon and nitrogen (POC and PON, respectively) and total bacteria count (TBC), in the main channel (orange column) and the tributaries (blue column) of the Ket River in spring flood and summer (early fall) baseflow.

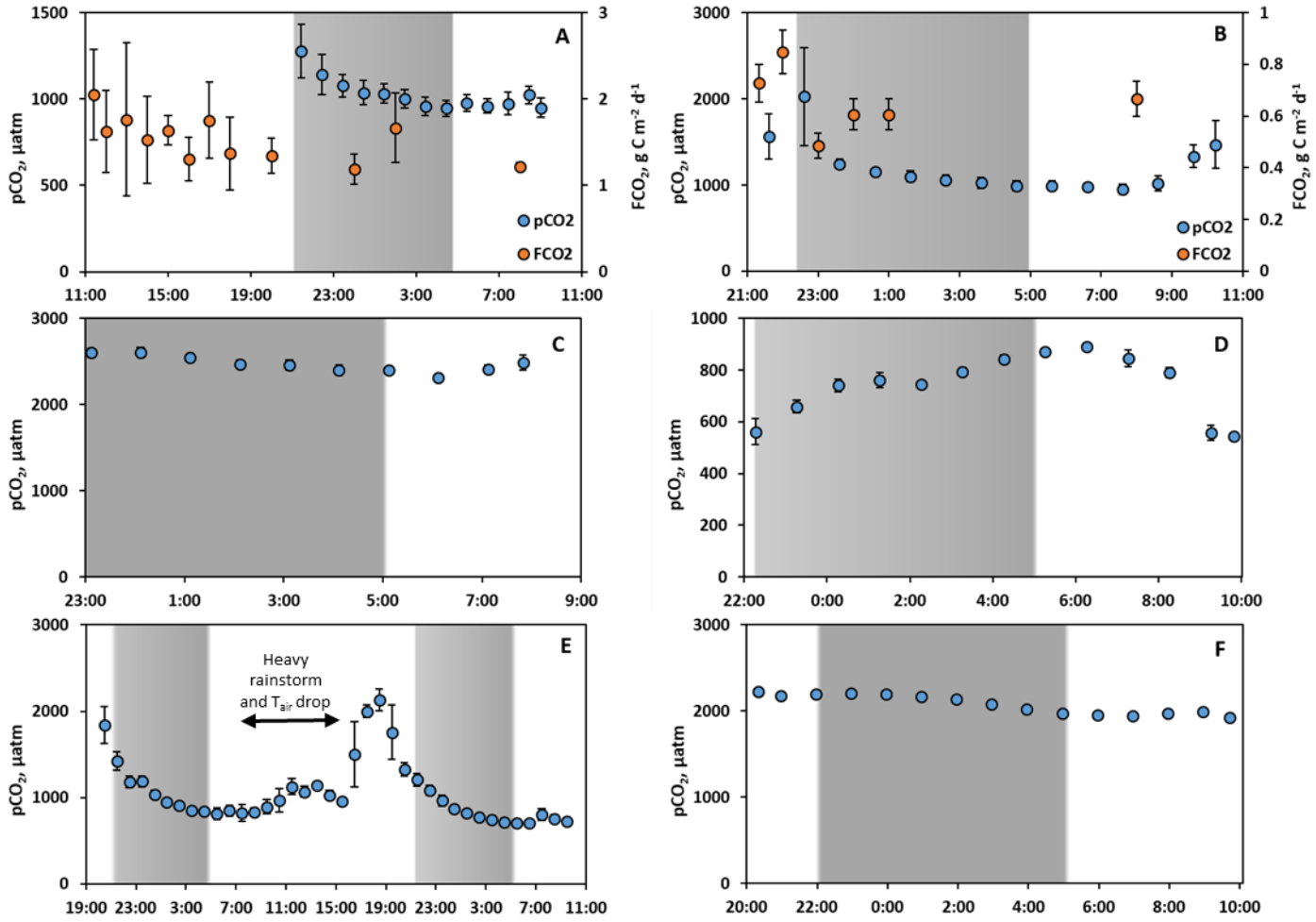

Figure 4. Continuous pCO_2 concentration (**A-F**, blue circles) and chamber-based fluxes (**A, B**) measured during spring flood period in tributaries (**A** Sochur No 3, **B** Lopatka No 8, **C** Derevyannaya No 12, **D** Ob river entrance, **E** Segondenka No 26) and in the Ket River main stem (middle course) near Stepanovka village (**F**) including night time measurements (shaded area). The measurement frequency was one per hour. Variations of water temperature were within the range of 0.3 to 0.6 °C and did not exhibit significant correlations with pCO_2 and FCO_2. Note that, for the small river Segondenka ($S_{watershed}$ = 472 km²), where the CO_2 peak was observed at 7 pm (**E**), there was quite heavy rainfall between 7 am and 3 pm.

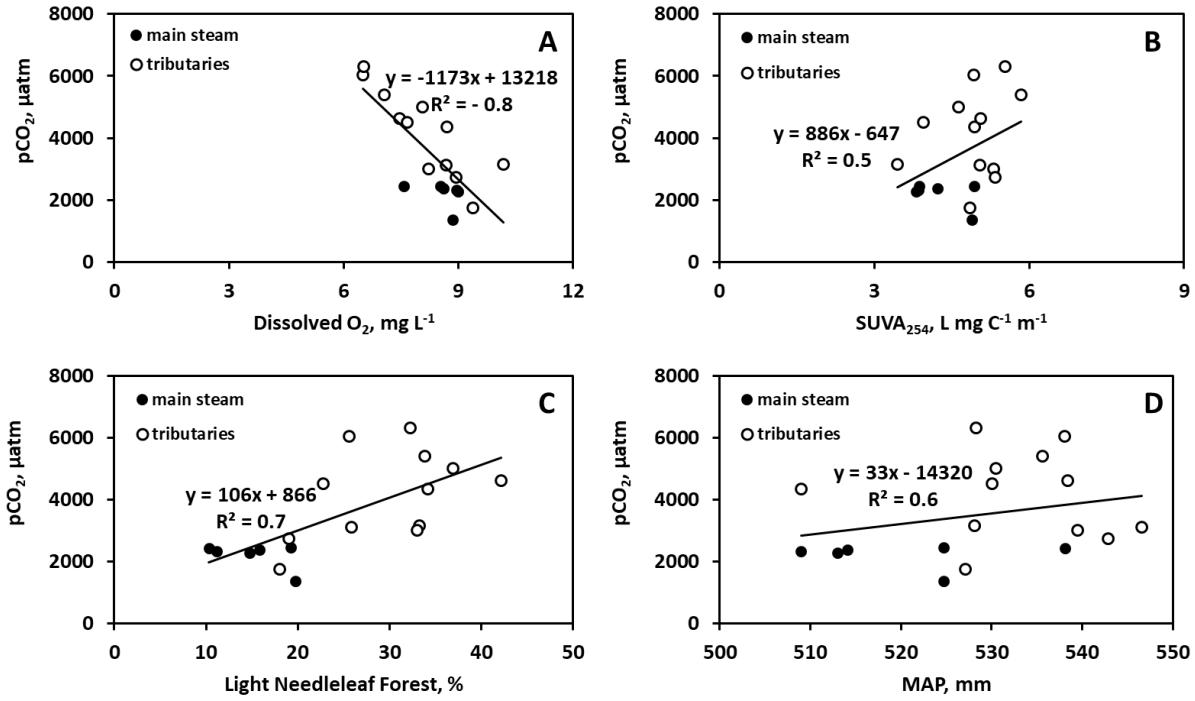

Figure 5. Significant ($p < 0.05$) control of dissolved oxygen (**A**), $SUVA_{254}$ (**B**), light needleleaf forest (**C**), and mean annual precipitation (**D**) on CO_2 concentration in the Ket River and tributaries during summer baseflow.